“Tantalum and Hydroxyapatite Particles Reinforced Magnesium for Biomedical and Load Bearing Application”

Tewodros Semeneh

A Thesis submitted to

Department of Materials Science and Engineering

School of Mechanical, Chemical and Materials Engineering

A Thesis Submitted in Partial Fulfillment of the Requirements for The Degree of MASTERS of Materials Science and Engineering

Office of Graduate Studies

Adama Science and Technology University

Adama, Ethiopia

June, 2018

“Tantalum and Hydroxyapatite Particles Reinforced Magnesium for Biomedical and Load Bearing Application”

Tewodros Semeneh

Advisor; Ass.prof. Jk KIM

Co-advisor; Ass.prof. H.C. Ananda Murthy

A Thesis submitted to

Department of Materials Science and Engineering

School of Mechanical, Chemical and Materials Engineering

A Thesis Submitted in Partial Fulfillment of the Requirements for The Degree of MASTERS of Materials Science and Engineering

Office of Graduate Studies

Adama Science and Technology University

Adama, Ethiopia

June, 2018

Approval sheet

To: ..... department

Subject: Thesis Submission

This is to certify that the thesis entitled "---------- ---------- submitted in partial fulfillment of the requirements for the degree of Master's in ----------, the Graduate program of the department of ----------, and has been carried out by ---------- Id. No ----------, under my supervision. Therefore, I recommend that the student has fulfilled the requirements and hence hereby he can submit the thesis to the department.

_____	_____	_____
Name of major Advisor	Signature	Date

Declaration

I hereby declare that this MSc Thesis is my original work and has not been presented for a degree in any other university, and all sources of material used for this thesis have been duly acknowledged.

Name: _____

Signature:_____

This MSc has been submitted for examination with my approval as thesis advisor

Name:_____

Signature:_____

Date of submission:……..

CONTENTS

ACKNOWLEDGMENTS

First, I would like to express my sincere gratitude to my Advisor Ass. Prof. Jk. KIM for his unlimited guidance, insight and suggestions throughout the research. I thank him from the bottom of my heart for introducing me to the area of composites. I thank him for his great patience, constructive criticism and myriad useful suggestions apart from invaluable guidance to me.

I am grateful to my co-advisor prof. H.C. Ananda Murthy for his encouragement and help to carry out the thesis work. I would also take this opportunity to express my gratitude and sincere thanks to Dr. Densfa Mensure, Head of Department of Materials science and Engineering for their invaluable advice, constant help, encouragement and inspiration.

I would take this opportunity to thank Mr. Demeke Tesfaye, Mr. Hentsa Laboratory (Technicians). I am also indebted to my colleagues for their unconditional support and constant motivation whenever needed. I am very grateful to all my dear friends who have given me their friendship, put up with my odd hours, and provided me with lifts and practical help. Last but not the least, I would like to thank my dear parents and my beloved Maki.

List of Tables

Tables **Page no.**

List of Figures

Figures **Page no.**

List of Acronyms and Abbreviations

Mg-magnesium

Ta-tantalum

HA-hydroxyapatite

Vol%-volume percent

Wt.%-weight percent

ρ-density

MMCs-Metal-matrix composites

MSRs- Mechanically induced self-sustaining reactions.

SHS-self-propagating high-temperature synthesis.

PM-powder metallurgy

YS-young's modulus

ES-elastic modulus

UCS-ultimate compression strength

FS-failure strain

LPSO-long period stacking ordered

BMG-bulk metallic glasses

DMEM-Dulbecco's modified Eagle's medium

OCP-open circuit potential

ROM-rule of mixture

CPP-

UTS-ultimate tensile strength

ABSTRACT

Pure magnesium (Mg) implants have unsatisfactory mechanical properties, particularly in loadbearing applications. Magnesium matrix composites reinforced with 3, 6, and 9 wt.% of Ta and 8wt. % of HA particles, which were sphere-like in shape with average size of about 60μm, were fabricated by powder metallurgy. The Density, porosity and mechanical properties of the composites were investigated. There were uniform distribution of reinforcements in the Mg matrix with reasonable integrity and no intermetallic formation. The compressive mechanical properties of composites vary with reinforcement contents. The obtained results showed that fine Ta and HA particles uniformly distribute in the Mg matrices without voids for the composites containing 3 and 6 wt.% Ta. For the composites containing 8 wt. % of HA and 9 wt.% Ta, however, Ta particles agglomerate in the Mg matrices, and some obvious voids appear. The ultimate compression strengths, Failure strain and elastic moduli of the composites tend to increase when the Ta contents increase from 0 to 6wt.%, however, appear to decrease with the further increase of Ta from 6 to 9 wt.%. But the yield strength was increased when the Ta reinforcement increased from 6 to 9 wt.%. The optimal parameters to fabricate biocompatible Mg composites and the optimal composition with appropriate strength, hardness and ductility were recommended.

Keywords: Powder metallurgy, magnesium composites, Tantalum, hydroxyapatite, Reinforcement

CHAPTER ONE

1.1 INTRODUCTION

Composites are an important group of engineering materials that contain a combination of two or more different materials with a clear interface between them. These distinct materials are referred to as matrix and reinforcement(s). The matrix can be either a metal, ceramic or polymer phase and the reinforcement (which can also be a metal, ceramic or polymer) is usually a different type of material from the matrix. Depending on the nature of the matrix, composites are known as metal-matrix composites if the matrix is a metal. Otherwise, they are known as polymer-matrix composites or ceramic-matrix composites [1].

The greatest advantage of the composites is that they combine the desirable properties of the matrix and the reinforcement. Accordingly, in metal-matrix composites that are reinforced with ceramic particles, the composites exhibit a higher yield strength and stiffness than the metallic matrix material, but also exhibit higher plasticity than the ceramic phase. Metal-matrix composites (MMCs) have been developed to combine the good ductility and toughness of the metal matrix and the superior strength and stiffness of the ceramic reinforcement, and they have been used in some important engineering applications including automotive and aerospace. MMCs reinforced by particles are of great interest since they exhibit properties, which are isotropic, easier to manufacture and often cheaper in comparison to the continuous fiber-reinforced MMCs. For most of the particulate MMCs, however, the sizes of the ceramic particles are typically in tens to hundreds of microns, resulting in considerable reduction in ductility and toughness and ineffective utilization of the strength and stiffness of the reinforcement. This is mainly due to the easy initiation and propagation of cracks in the ceramic particles or at the interface [2].

If enhanced mechanical properties are desired, very small particles must be used for reinforcement (1 μm or even smaller); a decrease of the reinforcement particle size leads to an increase in the mechanical strength of the composite [3]. The particle type, size, morphology, volume fraction, and distribution of reinforcing particles in the metal matrix play an important and critical role in enhancing or limiting the overall properties of the composite material.

Reinforcing the matrix with much smaller particles, in the submicron or Nano-sized range, is one of the key factors in producing high-performance composites, which yields improved mechanical properties [4].

Orthopedic biomaterials are generally limited to those materials that withstand cyclic loadbearing applications. While metals, polymers, and ceramics are used in orthopedics, it remains metals, which have over the years uniquely provided appropriate material properties such as high strength, ductility, fracture toughness, hardness, corrosion resistance, formability, and biocompatibility necessary for most loadbearing roles required in fracture fixation and total joint arthroplasty (TJA) [5].

Metallic materials continue to play an essential role as biomaterials to assist with the repair or replacement of bone tissue that has become diseased or damaged. Metals are more suitable for load-bearing applications compared with ceramics or polymeric materials due to their combination of high mechanical strength and fracture toughness Currently approved and commonly used metallic biomaterials include stainless steels, titanium and cobalt–chromium-based alloys. A limitation of these current metallic biomaterials is the possible release of toxic metallic ions and/or particles through corrosion or wear processes that lead to inflammatory cascades which reduce biocompatibility and cause tissue loss. Moreover, the elastic moduli of current metallic biomaterials are not well matched with that of natural bone tissue, resulting in stress shielding effects that can lead to reduced stimulation of new bone growth and remodeling which decreases implant stability. Current metallic biomaterials are essentially neutral in vivo, remaining as permanent fixtures, which in the case of plates, screws and pins used to secure serious fractures, must be removed by a second surgical procedure after the tissue has healed sufficiently [6].

Magnesium is an exceptionally lightweight metal. With a density of 1.74 g/cm3, magnesium is 1.6 and 4.5 times less dense than aluminum and steel, respectively [7]. Moreover, magnesium is essential to human metabolism and is naturally found in bone tissue. It is the fourth most abundant cation in the human body, with an estimated 1 mol of magnesium stored in the body of a normal 70 kg adult, with approximately half of the total physiological magnesium stored in bone tissue [8–10].

Magnesium-based materials were first introduced as orthopedic biomaterials in the first half of the century. The first use of magnesium was reported by Lambotte in 1907, who utilized a plate of pure magnesium (actual purity level unknown) with gold-plated steel nails to secure a fracture involving the bones of the lower leg. The attempt failed as the pure magnesium metal corroded too rapidly in vivo, disintegrating only 8 days after surgery and producing a large amount of gas beneath the skin. In an attempt to slow the corrosion process and increase the mechanical integrity of the implants, future in vivo works have investigated various magnesium alloys. Troitskii and Tsitrin, in 1944, reported on 34 cases where magnesium, alloyed with small levels of cadmium, was fashioned into plates and screws and used to secure various fractures. Of the 34 cases, 9 were unsuccessful; these failures were attributed to infection, or difficulties arising with the mounting of a plaster cast, which presumably did not allow for treatment of gas cysts. In all patients, no increase in serum levels of magnesium was observed. No distinct inflammatory reactions to the implant were observed. The material is reported to have stimulated the development of a hard callous at the fracture site. Hydrogen gas was given off in the corrosion process, however, was easily treated by drawing off the gas with a subcutaneous needle. While the sizes of the implants used were not given, it is reported that the mechanical integrity of most were maintained for 6–8 weeks, with complete resorption occurring in 10–12 months. On the contrary however, it was also reported that some implants only survived 3–5 weeks, which was attributed to increased acidity in the environment of some fractures [11-13].

The major drawback of magnesium in many engineering applications—its low corrosion resistance, especially in electrolytic, aqueous environments—becomes an intriguing property for biomaterial applications, where the in vivo corrosion of the magnesium-based implant involves the formation of a soluble, non-toxic oxide that is harmlessly excreted in the urine [14–17]. The unfortunate complication is that pure magnesium can corrode too quickly in the physiological pH (7.4–7.6) and high chloride environment of the physiological system, loosing mechanical integrity before the tissue has sufficiently healed and producing hydrogen gas in the corrosion process at a rate that is too fast to be dealt with by the host tissue. Moreover, due to functional roles and presence in bone tissue, magnesium may actually have stimulatory effects on the growth of new bone tissue [18,19,20].

Alloying, is one of the most common strategies to improve the mechanical properties as well as corrosion performance of metallic Mg [21]. So far, various alloying elements have been used and extensive investigations have been carried out on the composition design. But, most of the incumbent Mg alloys exhibit a certain degree of cytotoxicity and low corrosion resistance. Moreover, they possess low mechanical properties which are further reduced during degradation. Thus, they cannot mechanically endure and tolerate the activity of the patient for a significant time after implantation [22–26].

The addition of reinforcements to Mg matrix is an alternative technique, and this introduces a composite structure, resulting in improved mechanical properties, corrosion performance and wear resistance. High flexibility in component design and reinforcement material in composites also can rectify the biocompatibility of Mg [27,28,29]. Various types of reinforcements have been used in the Mg matrix over the past decades.

In medical applications, the biocompatibility and biodegradability of reinforcements needs to be considered. A few biocompatible reinforcements such as calcium, calcium polyphosphate, hydroxyapatite, Fluor apatite, titanium, niobium, have been used so far, while the properties and interaction of some with a Mg matrix have not been comprehensively investigated [30].

Milling is a significant unit operation in the many fields such as chemistry, pharmacy, mineral processing, and materials science. Many types of mills are employed in these fields and are ideally suited for wet or dry grinding processes, size reduction and dispersion, and deflocculation in solid–liquid systems. When a chemical reaction is produced during milling, the process is commonly referred to as mechanochemistry, and the mill device must be considered a reactor. Mechanochemistry is generally performed in high-energy ball mills using powder reactant mixtures. During milling, the intimate mixing of reactants and the continuous creation of fresh interfaces and defects enable the gradual progression of solid state reactions at room temperature. In many highly exothermic powder mixtures, ball milling can generate mechanically induced self-sustaining reactions (MSRs). An MSR process begins with an activation period, during which size reduction, mixing, and defect formation take place [31].

At a given milling time, called the ignition time (t_{ig}), a self-sustaining reaction is initiated and a reaction front propagates through the powder charge inside the vial [32]. The ignition time depends on the experimental conditions and the chemical system under investigation. MSR processes are comparable with self-propagating high-temperature synthesis (SHS), and they have similar requirements regarding the self-heating capacity of the mixtures. MSR processes is of fundamental importance because it can provide valuable information about the energy supplied by the milling devices during milling operations and the mechanisms of mechanochemical reactions.

MSR, in comparison to other mechanochemical processes, has the advantage of ignition time. This reproducible parameter can be measured by detecting the abrupt temperature increase of the milling vial or the total pressure inside the vial as a consequence of the heat released from the highly exothermic reaction. Ignition is a key moment in MSR that corresponds to a well-defined critical state of the powder reactants that is reached when the mill device has provided the net amount of energy necessary to generate a self-sustaining reaction [33].

The Mg matrix can be reinforced with biocompatible tantalum (Ta) particles through PM process. A few reports, to author's knowledge, about Mg-Ta composites are available from the literature. High strength Mg-Ta composites have been fabricated through powder metallurgy process [34]. They observed a uniform distribution of Ta particulates in the Mg matrix with no formation of intermetallic. Improved mechanical properties of Mg-Ta composites with addition of Ta up to 30 wt% hereafter have been reported. The peak hardness is achieved in 20% of reinforcement for Mg-Ta composites. This increment can be ascribed to addition of harder reinforcement materials to Mg matrix which restricts the local deformation of matrix during the indentation process [35].

1.2. Statement of the problems

Pure magnesium (Mg) implants have unsatisfactory mechanical properties, particularly in loadbearing applications. Mg may corrode too quickly in physiological and high chloride environments which leads to loss of mechanical integrity before sufficient healing of tissues.

Particulate-reinforced Mg composites are known as promising materials to provide higher strength implants compared to unreinforced Mg. low strength, high degree of shrinkage during solidification of molten Mg, high chemical reactivity especially at elevated temperatures have limited the use of Mg. Also, pure Mg has poor mechanical performance particularly in orthopedic applications.

1.3 Objective of the study

1.3.1 General objective of the study

The aim of this study is to investigate the effect of reinforcement on the densification, hardness and compressive strength of Mg-Matrix for biomedical application. The control sample (pure Mg) and Mg-based composite (Mg-Ta/HAp) were fabricated through mechanical alloying process using high energy planetary mill.

1.3.2 Specific objectives of the study

- Improve mechanical property (good ductility, strength, hardness, young's modulus).
- Evaluate particle distribution.
- Evaluation of density and porosity.
- Optimum composition of Ta and HA.

1.4 Significant of the study

- It contributes for bon medical clinics in Ethiopia
- It shows the other possible way Mg reinforced with hybrid (metal and ceramic) particles other than ceramics for load bearing application.
- It will have used as the initial input for further study in biomedical research.

CHAPTER TWO

2. LITRATURE REVIW

2.1 Magnesium properties and applications.

Magnesium is the lightest of all metals used as the basis for constructional alloys. It is this property which entices automobile manufacturers to replace denser materials, not only steels, cast irons and copper base alloys but even aluminum alloys by magnesium based alloys. The requirement to reduce the weight of car components as a result in part of the introduction of legislation limiting emission has triggered renewed interest in magnesium [36].

The growth rate over the next 10 years has been forecast to be 7% per annum. A wider use of magnesium base alloys necessitates several parallel programs. These can be classified as alloy development, process development/improvement and design considerations. The advantages of magnesium and magnesium alloys are; Lowest density of all metallic constructional materials, High specific strength, Good castability, suitable for high pressure die-casting; can be turned/milled at high speed, Good weldability under controlled atmosphere, Much improved corrosion resistance using high purity magnesium, Readily available, Compared with polymeric materials, Better mechanical properties, Resistant to ageing, Better electrical, thermal conductivity and Recyclable [37].

One of the reasons for the limited use of magnesium has been some poor properties exacerbated by a lack of development work. The disadvantages of magnesium are; Low elastic modulus, limited cold workability and toughness, limited high strength and creep resistance at elevated temperatures, high degree of shrinkage on solidification, high chemical reactivity, in some applications limited corrosion resistance [36].

The fracture toughness of magnesium is greater than ceramic biomaterials such as hydroxyapatite, while the elastic modulus and compressive yield strength of magnesium are closer to those of natural bone than is the case for other commonly used metallic implants (Table 1.1)

Table 1.1 Summary of the physical and mechanical properties of various implant materials in comparison to natural bone

Properties	Natural bone	Magnesium	Ti alloy	Co–Cr alloy	Stainless steel	Ta	Synthetic Hydroxyapatite
Density (g/cm^3)	1.8–2.1	1.74–2.0	4.4–4.5	8.3–9.2	7.9–8.1	16.65	3.1
Elastic modulus (Gpa)	3–20	41–45	110–117	230	189–205	186	73–117
Compressive yield strength (Mpa)	130–180	65–100	758–1117	450–1000	170–310	135-1060	600
Fracture toughness ($MPam^{1/2}$)	3–6	15–40	55–115	N/A	50–200	90-150	0.7

Compiled from references [7,38-41].

It is not possible to use conventional alloying techniques to improve some of the properties, e.g. elastic constants [42].

2.2 Reinforced magnesium composites by metallic particles for biomedical applications.

Pure magnesium (Mg) implants have unsatisfactory mechanical properties, particularly in loadbearing applications. Particulate-reinforced Mg composites are known as promising materials to provide higher strength implants compared to unreinforced metals. In the current work biocompatible niobium (Nb) and tantalum (Ta) particles are selected as reinforcement, and Mg-Nb and Mg-Ta composites fabricated via a powder metallurgy process associated with the ball milling technique [43].

The effect of Nb and Ta contents on the microstructure and mechanical properties of Mg matrix was investigated. There was a uniform distribution of reinforcements in the Mg matrix with reasonable integrity and no intermetallic formation. The compressive mechanical properties of composites vary with reinforcement contents. The optimal parameters to fabricate biocompatible Mg composites and the optimal composition with appropriate strength, hardness and ductility are recommended [44].

The microhardness of pure Mg, Mg-Nb and Mg-Ta composites are illustrated in Fig. 1.1 The average microhardness of Mg composites was increased with increasing the content of reinforcement material. The microhardness experiments reveal a maximum increase of about 21% and 15% in Mg-Nb and Mg-Ta composites, respectively, comparing to pure Mg. The peak hardness is achieved in 20% of reinforcement for both Mg-Nb and Mg-Ta composites. This increment can be ascribed to addition of harder reinforcement materials to Mg matrix which restricts the local deformation of matrix during the indentation process. The microhardness results of currently investigated Mg composites is consistent with other metallic and ceramic reinforced Mg composites [35].

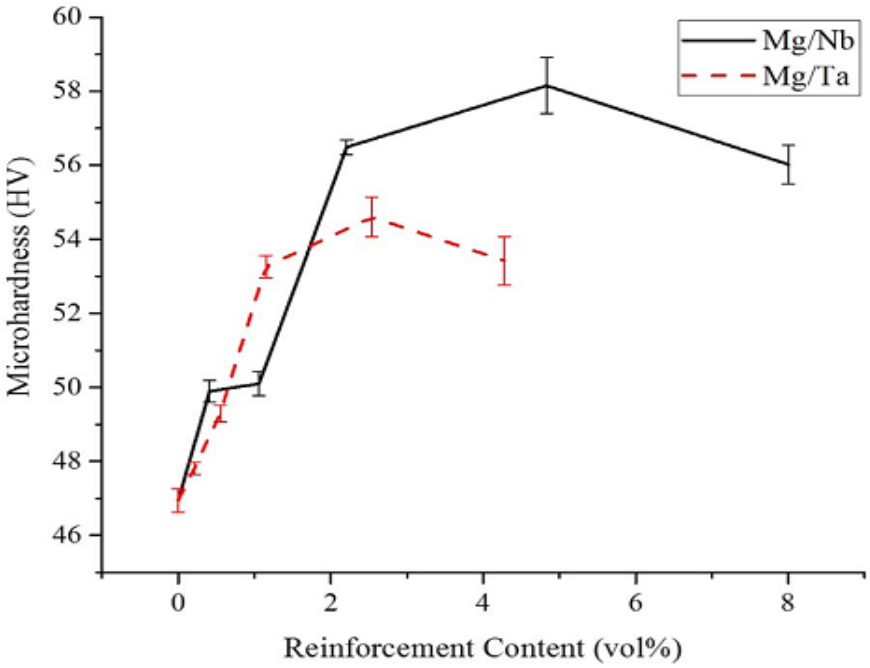

Figure 1.1 Microhardness of pure Mg, Mg-Nb and Mg-Ta composites [35].

Continuous fibers were early materials used as reinforcement in Mg matrix; however, they were then substituted by discontinuous fibers and whiskers due to some restrictions such as cost of continuous fibers and limited fabricability and availability. Particles are receiving increasing attention as an alternative type of reinforcement and are currently used commercially [45].

Up till now, three routines have been developed to solve the fast degradation rate of magnesium and its alloys. One is alloying magnesium with non-toxic elements such as Ca [46], Zn and Zr [47] to form novel magnesium alloys. The second is surface modification of traditional magnesium alloys, such as coating Ca–P [48], bonelike apatite [49], brushite [50], hydroxyapatite [51,52] layers on the alloys. An alternative routine is to form magnesium-matrix composite reinforced with bioactive ceramic. Recently, [53] reported a potential of AZ91D magnesium-matrix composites reinforced with hydroxyapatite (HA) particles for load-bearing applications. In this magnesium-matrix composites, however, the AZ91D matrix contains toxic element Al which appears to be the impairment of phosphorous metabolism and its resultant adverse effects [54]; and also HA is a bio ceramic with slow degradation rate, there being a risk that the HA particles remained from the completely degraded matrix could react with macrophages resulting in bone osteolysis [55]. The choice of reinforcement is dictated by several factors such as application, manufacturing method and cost of fabrication in medical applications, the biocompatibility and biodegradability of reinforcements needs to be considered. A few biocompatible reinforcements such as calcium, calcium polyphosphate, hydroxyapatite, fluorapatite, titanium, niobium, have been used so far, while the properties and interaction of some with a Mg matrix have not been comprehensively investigated [56,57,58].

Pure titanium (Ti) particulate reinforced pure magnesium (Mg) composite materials were fabricated via powder metallurgy route, and their microstructural and mechanical properties were evaluated. When using the elemental mixture of pure Mg and pure Ti powders and consolidating them by solid-state sintering process, no significant increase in tensile strength of the composites was obtained, because of poor bonding strength at the interface between -Mg matrix and Ti particles [59].

In particular, coarse magnesium oxide (MgO) particles of about 100 nm were formed via thermite reaction between TiO_2 surface films of Ti particles and Mg raw powders and resulted in preventing the improvement of the mechanical properties of the composite material. On the other hand, when using the atomized pure Mg composite powders reinforced with Ti particulates, their extruded composite material showed obviously improved tensile strength and good elongation, compared to the extruded pure Mg powder material including no Ti particle [59,60].

The obvious improvement in the tensile strength was due to the restriction of dislocation movement by Ti reinforcements under applied tensile load. The stress–strain curves of these composites in compression test are shown in Fig. 1.2 Each fabricated composite material indicates a plateau region at about 125–130 MPa in the compression stress, and obviously the remarkable increase of the stress following the plateau region. The Mg–5-mass% Ti composite indicates the fractured stress of 418 MPa, which is a little higher than that of pure Mg (403 MPa) [61].

The total strain of the former is significantly small compared to the extruded pure Mg reinforced with no Ti particle. Furthermore, as shown in Fig.1.2, the increase and its following decrease of the compression stress, which is similar to the upper yielding of the conventional steel, occurs at the magnified region before the plateau.

A very slight increase of the maximum compression strength occurs with increase in the content of Ti particle reinforcements. Mg–5-mass% Ti composite material also indicates a higher plateau stress of about 130 MPa compared to the other specimens. When the compressive load is applied, the stress transfer between Ti particles and -Mg matrix is active and results in the increase of the yield and plateau stress due to the higher hardness of Ti particles than pure Mg matrix [60].

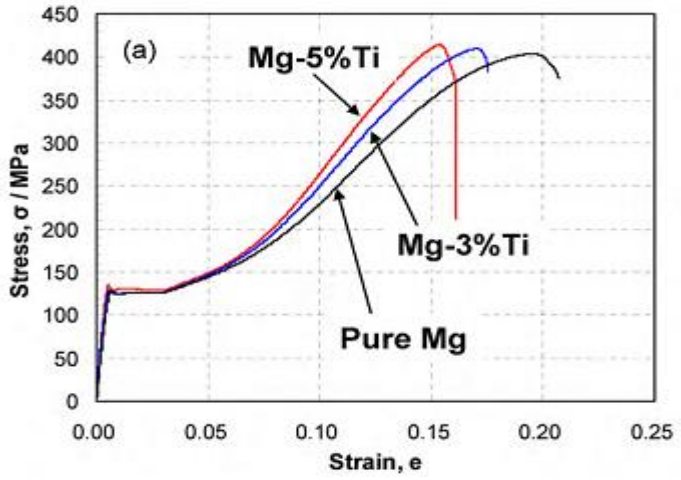

Figure 1.**2** Stress–strain curves in compression test at room temperature of hot extruded Mg composite materials reinforced with Ti particles by using elemental mixture powders (Ti content: 0 mass%, 3 mass%, and 5 mass%) [60].

Magnesium based composites containing 5–15 wt% niobium particulates were synthesized using disintegrated melt deposition technique. Microstructural characterization revealed reasonably uniform distribution of niobium particulates in the matrix with no inter metallic formation, reasonable grain refinement and minimal porosity.

Mechanical characterization under tensile loading revealed simultaneous improvement in hardness, 0.2% yield strength and ultimate tensile strength up to 10 wt% Nb, while ductility was compromised beyond 5 wt% niobium particulate addition to pure magnesium. The optimal composition with good combination of strength and ductility is observed at Mg/5 wt% Nb composite while the best improvement in strength and hardness among the composites was observed only for Mg–10 wt% Nb composite [62].

Metallic materials continue to play an essential role as biomaterials to assist with the repair or replacement of bone tissue that has become diseased or damaged. Metals are more suitable for load-bearing applications compared with ceramics or polymeric materials due to their combination of high mechanical strength and fracture toughness. Currently approved and commonly used metallic biomaterials include stainless steels, titanium and cobalt–chromium-based alloys [63].

A limitation of these current metallic biomaterials is the possible release of toxic metallic ions and/or particles through corrosion or wear processes that lead to inflammatory cascades which reduce biocompatibility and cause tissue loss. Moreover, the elastic moduli of current metallic biomaterials are not well matched with that of natural bone tissue, resulting in stress shielding effects that can lead to reduced stimulation of new bone growth and remodeling which decreases implant stability. Current metallic biomaterials are essentially neutral in vivo, remaining as permanent fixtures, which in the case of plates, screws and pins used to secure serious fractures, must be removed by a second surgical procedure after the tissue has healed sufficiently [64].

Magnesium is essential to human metabolism and is naturally found in bone tissue. It is the fourth most abundant cation in the human body, with an estimated 1 mol of magnesium stored in the body of a normal 70 kg adult, with approximately half of the total physiological magnesium stored in bone tissue. Magnesium is a co-factor for many enzymes, and stabilizes the structures of DNA and RNA. The level of magnesium in the extracellular fluid ranges between 0.7 and 1.05 mmol/L, where homeostasis is maintained by the kidneys and intestine [65].

While serum magnesium levels exceeding 1.05 mmol/L can lead to muscular paralysis, hypotension and respiratory distress, and cardiac arrest occurs for severely high serum levels of 6–7 mmol/L, the incidence of hyper-magnesium is rare due to the efficient excretion of the element in the urine. The major drawback of magnesium in many engineering applications—its low corrosion resistance, especially in electrolytic, aqueous environments—becomes an intriguing property for biomaterial applications, where the in vivo corrosion of the magnesium-based implant involves the formation of a soluble, non-toxic oxide that is harmlessly excreted in the urine. Moreover, due to functional roles and presence in bone tissue, magnesium may actually have stimulatory effects on the growth of new bone tissue [63,64]. Thus, it is projected that magnesium and its alloys be applied as lightweight, degradable, load bearing orthopedic implants, which would remain present in the body and maintain mechanical integrity over a time scale of 12–18 weeks while the bone tissue heals, eventually being replaced by natural tissue [66].

The microstructural evolution and mechanical properties of extruded Mg composites containing micro-Ti particulates hybridized with varying contents of nano-B4C are investigated, and compared with Mg-5.6Ti. Microstructural characterization showed the presence of uniformly distributed micro-Ti particles embedded with nano-B4C particulates that resulted in significant grain refinement. Electron back scattered diffraction (EBSD) analyses of Mg-(5.6Ti + x-B_4C) BM hybrid composites showed that the addition of hybridized particle resulted in relatively more recrystallized grains, realignment of basal planes and extension of weak basal fiber texture when compared to Mg-5.6Ti [67].

The evaluation of mechanical properties indicated improved strength with ductility retention in Mg-(5.6Ti + x-B_4C) BM hybrid composites. When compared to Mg-5.6Ti, the superior strength properties of the Mg-(5.6Ti+ x-B_4C) BM hybrid composites are attributed to the presence of Nano-reinforcements, the uniform distribution of the hybridized particles, better interfacial bonding between the matrix and the reinforcement particles and the matrix grain refinement achieved by nano-B_4C addition. The ductility enhancement obtained in hybrid composites can be attributed to the fiber texture spread and favorable basal plane orientation achieved due to Nano B_4C addition [62,68].

The flow curves of developed Mg-materials under compressive loading are shown in Fig.1.3 It clearly indicates the superior strength properties of developed Mg materials (in comparison with pure Mg) and the strengthening effects from individual Ti and hybrid (5.6Ti + x-B4C)$_{BM}$ reinforcements. the yield strength and ultimate strength of Mg-(5.6Ti + x-B4C) $_{BM}$ composites are found to increase with the increase in B4C addition and amongst the composites, Mg-(5.6Ti + 2.5B4C) $_{BM}$ composite exhibit the highest strengths [68].

The strength properties improvement in Mg-(5.6Ti + x-B4C) $_{BM}$ composites as mentioned above can primarily be ascribed to the presence and relatively uniform distribution of hybrid (5.6Ti + x-B4C) $_{BM}$ reinforcements/second phases and the combined presence of Ti (B, C) intermetallic phases at the Mg/Ti interface [69].

In the Mg-(5.6Ti + x-B4C) $_{BM}$ composites, the dominant strengthening mechanisms are the coupled effects of (i) the presence of fine hybrid reinforcement/intermetallic phases and the effective load transfer from matrix to second phases and (ii) the grain refinement due to localized dynamic recrystallization [70].

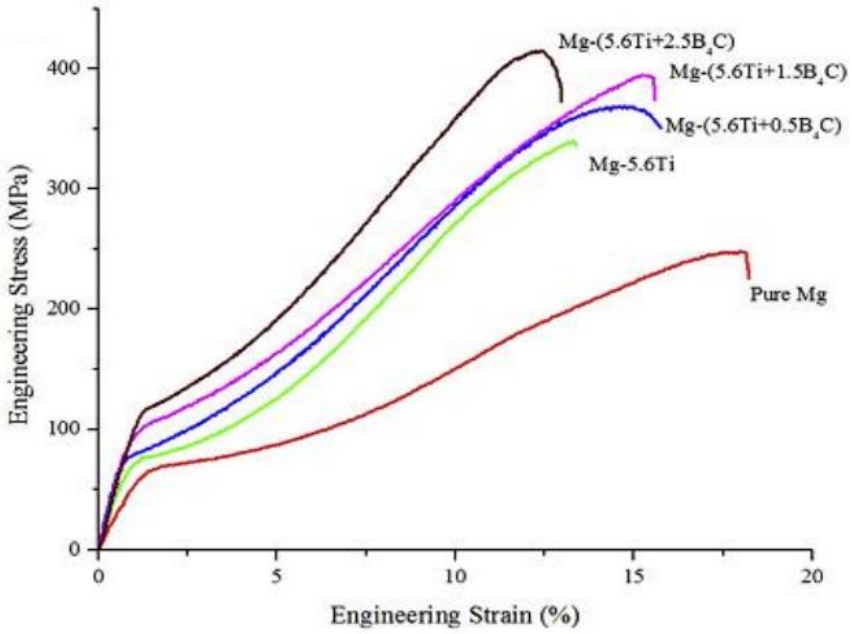

Figure 1.3 compressive response of developed Mg materials [70].

2.3 Reinforced magnesium composites by ceramics particles for biomedical applications.

Magnesium alloy (ZK60A) matrix composite s reinforced with 2.5, 5, 7.5 and 10 wt.% calcium polyphosphate particles, which were sphere-like in shape with average size of about 750 nm, were fabricated by powder metallurgy. The microstructure, mechanical properties and degradation behavior in physiological saline of the composites were investigated. The obtained results show that ultrafine calcium polyphosphate particles uniformly distribute in the ZK60A matrices without voids for the composites containing 2.5 and 5 wt.% calcium polyphosphate. For the composites containing 7.5 and 10 wt.% calcium polyphosphate, however, calcium polyphosphate particles agglomerate in the ZK60A matrices, and some obvious voids appear [71].

The ultimate tensile strengths, yield strengths and elastic moduli of the composites tend to increase when the calcium polyphosphate contents increase from 0 to 5 wt.%, however, appear to decrease with the further increase of calcium polyphosphate from 5 to 10 wt.%. The weight losses of the composites, pH values and Mg ion concentrations of the solutions immersing the composites gradually decrease with increase of calcium polyphosphate content, which indicates that the addition of more calcium polyphosphate into ZK60A alloy results in significant degradation slow-up of the composites. This can be attributed to the formation of dense corrosion product layers on the composites. The composites have good mechanical properties and controllable degradation rates and thereby have potential to be used as load- bearing bone implants [72,73].

The effect of CPP content on the mechanical properties of the CPP p/ZK60A composites. As shown in Fig.1.4 the ultimate tensile strengths (UTS), yield strengths (YS) and elastic moduli (E) of the composites tend to increase when the CPP contents increase from 0 to 5 wt.%, however, appear to decrease with the further increase of CPP from 5 to 10 wt.%. The maximum UTS and YS, obtained from the 5 wt.% CPP-containing composite, are about 337.4 MPa and 319.5 MPa, higher than those of ZK60A by 21.4% and 30.5%, respectively[74].

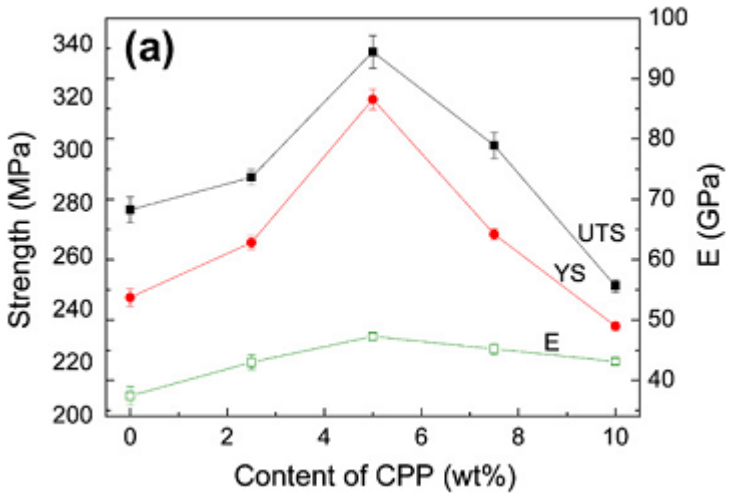

Figure 1.4 The tensile properties including the ultimate strength (UTS), yield strength (YS) and elastic modulus (E) of the composites with different CPP contents [74].

Room temperature mechanical properties of pure magnesium, Mg/ZrO_2 and Mg/ (ZrO_2 + Cu) composites with various compositions are investigated. Results revealed that the use of hybrid (ZrO_2 + Cu) reinforcements in Mg led to enhanced mechanical properties when compared to that of single reinforcement (ZrO_2) [75].

Marginal reduction in mechanical properties of Mg/ZrO_2 composites were observed mainly due to clustering of ZrO_2 particles in Mg matrix and lack of matrix grain refinement. Addition of hybrid reinforcements led to grain size reduction and uniform distribution of hybrid reinforcements, globally and locally, in the hybrid composites. Macro- and micro- hardness, tensile strengths and compressive strengths were all significantly increased in the hybrid composites. With respect to unreinforced magnesium, failure strain was almost unchanged under tensile loading while it was reduced under compressive loading for both Mg/ZrO_2 and Mg/ (ZrO_2 + Cu) composites [76].

Biomedical metals are widely used as implants. However, medical metals such as stainless steel and titanium alloys can result in stress shielding of the bone and these permanent implants need to be removed by a secondary surgery after healing. Biomedical polymers are degradable but they do not have sufficient mechanical strength. As a result, application of these materials is limited and new biodegradable materials are needed. Mg-Zn-Y alloys with a long period stacking ordered (LPSO) phase are potential candidates for biodegradable implants; however, an unfavorable degradation rate has limited their applications [77].

Hydroxyapatite (HA) has been shown to enhance the corrosion resistance of Mg alloys. $Mg_{97}Zn_1Y_{2-0.5}$ wt% HA composite was synthesized and solution treated at 500 ˚C for 10 h. The corrosion behavior of the composite was studied by electrochemical and immersion tests, while the mechanical properties were investigated by a tensile test. Addition of HA particles improves the corrosion resistance of $Mg_{97}Zn_1Y_2$ alloy without sacrificing tensile strength [75,76].

The improved corrosion resistance is due to the formation of a compact Ca-P surface layer and a decrease of the volume fraction of the LPSO phase, both resulting from the addition of HA. After solution-treatment, the corrosion resistance of the composite decreases. This is due to the formation of a more extended LPSO phase, which weakens its role as a corrosion barrier in protecting the Mg matrix.

Table 2**.1** Volume fraction of phases, grain size, Vickers hardness, and tensile properties of the tested alloys. Yield strength (YS), ultimate tensile strength (UTS), long period stacking ordered (LPSO) [78].

Sample	α-Mg (%)	LPSO (%)	Grain Size (μm)	YS (MPa)	UTS (MPa)	Elongation (%)
MgZnY-C	75.1	24.9	243 ± 10	126 ± 13	172 ± 9	9.0 ± 0.6
MgZnY-T	77.8	22.2	254 ± 16	108 ± 6	179 ± 3	14.0 ± 2.4
HA-C	82.3	17.7	232 ± 19	117 ± 2	161 ± 2	9.2 ± 0.2
HA-T	82.2	17.8	241 ± 7	109 ± 9	163 ± 18	12.0 ± 5.6

The volume fraction of the phases, yield strength (YS), ultimate tensile strength (UTS), and elongation of the as-cast and solution treated alloys are given in Table 2.1 The volume fraction of the LPSO phase decreases from 24.9% in the MgZnY-C alloy to 17.7% in the HA-C alloy. YS and UTS of the MgZnY-C alloy are 126 and 172 MPa, respectively, while the YS and UTS of the HA-C alloy are 117 and 161 MPa, respectively. With the addition of HA, YS, and UTS of the MgZnY alloy decrease slightly. According to the Hall-Patch equation, the strength increases as the grain size decreases. The grain refinement in the HA-C alloy is expected to increase the strength as compared with that of MgZnY-C alloy. The hardness value of the LPSO phase (118 HV) is higher than that of α-Mg (73 HV) in the MgZnY-C alloy. As a result, the role of the LPSO phase in tested alloys can be treated as reinforcement while α-Mg can be seen as the matrix in the alloy [75,77].

The YS and UTS are expected to decrease with the decrease in the volume fraction of the LPSO phase. However, the differences of the YS and UTS values between the MgZnY-C and HA-C alloys are small even though the volume fraction of the LPSO phase is lowered in the HA-C alloy. This is most likely due to the grain size strengthening in the HA-C alloy, which compensates the negative effect resulting from the decrease of LPSO phase in the HA-C alloy. Thus, no sharp decrement of mechanical properties is observed although the volume fraction of LPSO phase is lowered after the addition of HA. YS and UTS of the MgZnY-T alloy are 108 and 179 MPa, respectively, while the YS and UTS of the HA-T alloy are 109 and 163 MPa, respectively. YS values of the alloys decrease slightly after solution treatment (Table 2.1).

The effect of solution-treatment on the mechanical properties can be discussed based on grain size, and volume fraction, morphology, distribution and type of LPSO phase. A slight grain growth is observed in the solution-treated alloys, which has a negative effect on the strength [78].

There have been vast advances in the field of biomaterials, including ceramics, glasses, glass-ceramics and metal alloys. Dense and porous ceramics have been widely used for various biomedical applications. Current applications of bio ceramics include bone grafts, spinal fusion, bone repairs, bone fillers, maxillofacial reconstruction, *etc*. Amongst the various calcium phosphate compositions, hydroxyapatite, which has a composition similar to human bone, has attracted wide interest. Much emphasis is given to tissue engineering, both in porous and dense ceramic forms.

The various applications of dense hydroxyapatite and other dense biomaterials on the aspects of transparency and the mechanical and electrical behavior. Prospective future applications, established along the aforesaid applications of hydroxyapatite, appear to be promising regarding bone bonding, advanced medical treatment methods, improvement of the mechanical strength of artificial bone grafts and better *in vitro*/*in vivo* methodologies to afford more particular outcomes [79].

2.4 The effects of processing techniques on magnesium-based composite

The reinforcements, matrix materials and properties of composites are very sensitive to fabrication method. There are two major methods to produce particle-reinforced Mg composites: powder metallurgy (PM) and molten methods. In the molten method, some parameters such as high activity of molten Mg, lack of wettability of some particles by molten Mg and reactivity of some reinforcements with molten Mg have to be taken into consideration. However, the powder metallurgy method, implemented at low temperatures, is appropriate for highly reactive and low wettable reinforcements and Mg matrix. Moreover, the higher flexibility in reinforcement material, feasibility to utilize high volume fractions of reinforcements of up to 50% and higher available homogeneity have developed PM as a promising technique in Mg composite fabrication [80,57,81].

Owing to the advantages of magnesium as a biomaterial, study on synthesis of magnesium materials is of prime importance. This chapter introduces potential synthesis techniques for synthesizing both impermeable and porous magnesium-based biomaterials.

Primary processing of magnesium-based materials (alloys and composites) can be classified into liquid-state and solid-state processes. Even though there are many synthesizing methodologies for magnesium-based alloys and composites, very few were adopted for synthesizing biomaterials, especially porous magnesium materials. Recent technology advancements enable the researchers and engineers to synthesize homogeneous magnesium alloys and composites utilizing high-purity raw materials and continuously strive to achieve repeatability of material properties at all times [57,81].

The most common solid-state processing technique for synthesizing magnesium based materials is powder metallurgy (PM) technique. Raw material (metal or ceramic) in the form of powders is formed into specific shape and subsequently sintered at a temperature just below the melting temperature of the primary constituent (magnesium) of the powder mixture. PM technique has the capability of forming near-net-shaped products. Initial stage of this PM technique is blending where the powders (raw material) are mixed homogeneously. The blending conditions mostly depend on the density difference between the constituents of the powder mixture. After blending, cold press or hot press or hot isostatic press is employed to produce a “green compact,” which is about 80 % dense and then followed by sintering. Sintering should be effective enough to improve

the bonding between the powders and thereby to minimize porosity. It can be done by using a traditional resistance heating furnace where the direction of heating is from outside to inside of the powder compact resulting in poor microstructural characteristics of the core of the material [80,81].

Microwave can also be utilized to sinter the green compact where both electric and magnetic field act together to sinter the compact. When compared to the conventional sintering, heating in microwave sintering is able to achieve comparably higher densities. Desirable properties of materials can be achieved through microwave sintering due to the following:

(a) Shorter sintering time and
(b) Lower sintering temperatures.
Unlike in traditional heating, the direction of heating in microwave is from inside to outside of the powder compact which results in poor microstructural characteristics of the surface [82].

There has been growing interest in the development of metal matrix composites (MMCs) for the aerospace industry because of their attractive physical and mechanical properties and enhanced elevated temperature capabilities. However, some of the fabrication techniques (e.g. using powder metallurgy) for this new class of MMCs are hampered by (i) the poor distribution of the reinforcements, and (ii) the limited room temperature ductility of the composites and hence formability. This presentation reports work done to address the above two problems by (i) an analysis based on size difference of matrix and reinforcement particles, taking into account the processing parameters, and (ii) introducing an innovative way of extruding brittle composites to increase its formability [83].

Powder metallurgy (P/M) aluminum-based composites reinforced by ceramic particles such as SiC, Al 2O3, Si3N4, etc., have been widely reported. The reinforcement sizes and volume fractions, which are important criteria in the resultant microstructure and properties, seem to be determined randomly or by experience, and are not parameter-based and/or do not follow any fixed rule. In normal instances, in order to increase the strength and ductility, fine reinforcements and a relatively large volume fraction are preferred. However, it is difficult to take advantage of both these requirements because they are prone to cause an inhomogeneous distribution. Poor distribution of reinforcement degrades the composites in terms of its physical and mechanical properties and negates the attractiveness of reinforcement additions [84,85].

The conventional P/M route for making MMCs includes:

1. mixing and blending

2. consolidation, e.g. hot pressing

3. secondary processing e.g. extrusion, rolling

Theoretically, when secondary processing with a large enough deformation is introduced, homogeneous distribution of reinforcements could be achieved regardless of the size difference between matrix powder and reinforcement particle [85].

Composites containing pure magnesium and hybrid reinforcements (5.6 wt.% titanium (Ti) particulates and 2.5 wt.% nanoscale alumina (n-Al_2O_3) particles) were synthesized using the disintegrated melt deposition technique followed by hot extrusion. The hybrid reinforcement addition into the Mg matrix was carried out in two ways: (i) by direct addition of the reinforcements into the Mg–matrix, Mg– (5.6Ti + 2.5n-Al_2O_3) and (ii) by pre-synthesizing the composite reinforcement by ball milling and its subsequent addition into the Mg–matrix, Mg–(5.6Ti + 2.5n-Al2O3) BM. Microstructural characterization revealed significant grain refinement due to reinforcement addition [86].

The evaluation of mechanical properties indicated a significant improvement in micro hardness, tensile and compressive properties of the composites when compared to monolithic magnesium. For the Mg– (5.6Ti + 2. 5n-Al_2O_3) composite, wherein the reinforcements were directly added into the matrix, the improvement in strength properties occurred at the expense of ductility. For the Mg– (5.6Ti + 2. 5n-Al_2O_3) BM composites with pre-synthesized ball-milled reinforcements, the increase in strength properties was accompanied by an increase/retention of ductility. The observed difference in behavior of the composites is primarily attributed to the morphology and distribution of the reinforcements obtained due to the ball-milling process, thereby resulting in composites with enhanced toughness [87].

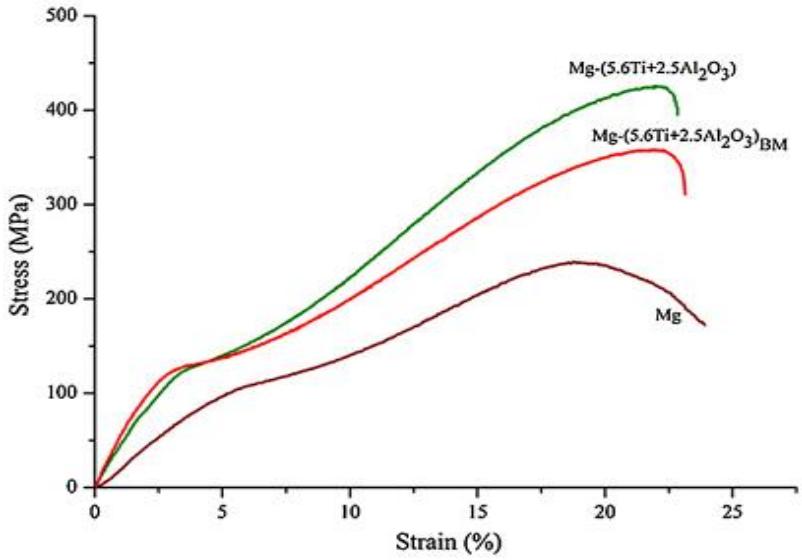

Figure 1.5 Compressive stress–strain curves of monolithic Mg and its hybrid composites [88].

The compression test results as shown in Fig 1.5 indicate an increase of >20% in the compressive yield strength (0.2% CYS) and >45% in ultimate compressive strength (UCS) for both the composites. The work of fracture of the composites also improves significantly when compared to monolithic Mg. The hybrid composite incorporated with the direct additions of reinforcements show better overall compressive strength properties than the hybrid composite reinforced with ball milled reinforcements [88].

The effect of processing techniques on the densification, hardness and compressive strength of Mg alloy and Mg-based composite for biomaterial application. The control sample (pure Mg) and Mg-based composite (Mg-Zn/HAp) were fabricated through mechanical alloying process using high energy planetary mill, whilst another Mg-Zn/HAp composite was fabricated through double step processing (the matrix Mg-Zn alloy was fabricated by planetary mill, subsequently HAp was dispersed by roll mill) [90]. Mechanical properties of the sintered pellets were characterized by microhardness and compression test. The results show that the density of the pellets was significantly increased by addition of HAp, but the most optimum density was observed when the sample was fabricated through double step processing (1.8046 g/cm3). Slight increment in hardness and ultimate compressive strength were observed for Mg-Zn/HAp composite that was fabricated through double step processing (58.09 HV, 132.19 MPa), as compared to Mg-Zn/HAp produced through single step processing (47.18 HV, 122.49 MPa) as shown in Fig 1.6

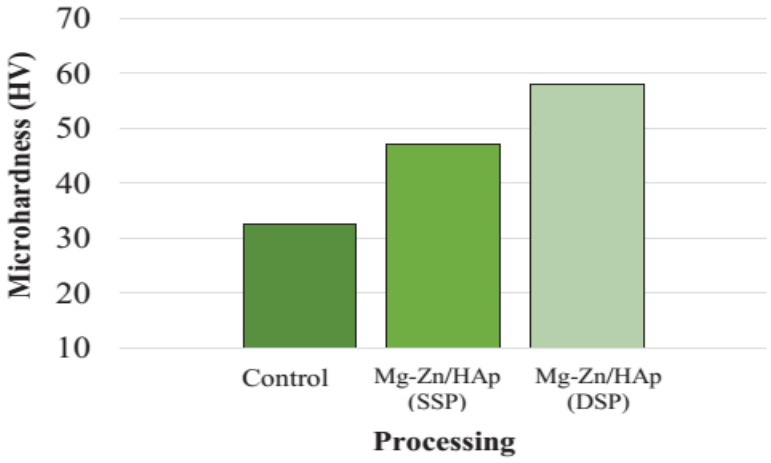

Figure 1.6. Microhardness of the control and Mg-Zn/HAp composite [90].

The result of compressive strength of the respective control and magnesium-based composite have been presented in Figure 1.7 Ultimate compressive strength of the control sample was found to be as low as 122.74 MPa and surprisingly to be approximately equal to the Mg-Zn/HAp composite that was processed through single step processing (planetary mill) (122.49 MPa). However, Mg-Zn/HAp that was processed through double step processing appeared to have an increment in the compressive strength (132.19 MPa). This increment is contributed mainly by the particle size of the composite. Generally, reinforcing particles may produce an increase in the ultimate compressive strength of a composite when subjected to compression test, where compression tends to close cracks and flaws that are perpendicular to the applied stress, and therefore increase the compressive strength [89,90]. However, the strength of two-phase composites is still highly relying on the effectiveness of stress transfer between the matrix and the reinforcement. For poorly bonded particles, the stress transfer at the interface of particles/matrix is inefficient, thus caused the destruction in compressive strength, as can be observed for SSP Mg-Zn/HAp. Since the HAp particles is dispersed in the Mg-Zn matrix separately in the fabrication process of Mg-Zn/HAp (DSP), the particle size of the resultant composite tends to be much smaller, thus increase the surface contact area and the efficiency of the stress transfer between the matrix and the reinforcing HAp. DSP aided the dispersion of hydroxyapatite to be homogeneously dispersed into the matrix of Mg-Zn [90].

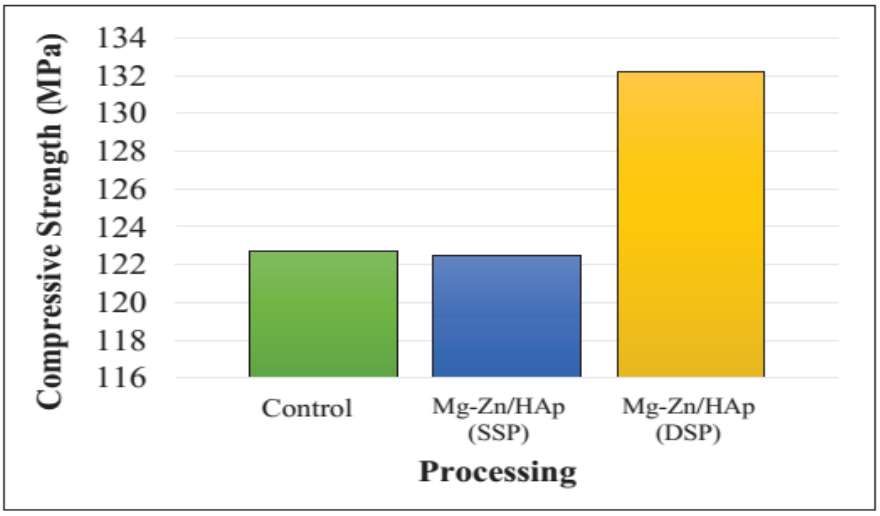

Figure 1.7 Compressive strength of the control and Mg-Zn/HAp composite fabricated through two techniques [90].

2.5 Reinforced magnesium based composites to improve mechanical properties.

Magnesium (Mg) composite reinforced with carbon nanotubes (CNTs) having superior mechanical properties was fabricated using both pure Mg and AZ61 Mg alloy matrix [92]. The composites were produced via powder metallurgy route containing wet process using isopropyl alcohol (IPA) based zwitterion surfactant solution with unbundled CNTs [91,92].

The produced composites were evaluated with tensile test and Vickers hardness test and analyzed by X-ray diffraction (XRD) and field-emission scanning electron microscopy (FE-SEM) equipped with energy dispersive spectroscopy (EDS) and electron back scattered diffraction (EBSD). As a result, only with AZ61 Mg alloy matrix, tensile strength of the composite was improved. In situ formed Al_2MgC_2 compounds at the interface between Mg matrix and CNTs effectively reinforced the interfacial bonding and enabled tensile loading transfer from the Mg matrix to nanotubes. Furthermore, it was clarified that the microstructures and grain orientations of the composite matrix were not significantly influenced by CNT addition [92].

Elongation of these composites was extremely reduced to less than 5%, yield stress at 0.2% offset of pure Mg with 1.10 vol% curving type CNTs, with 1.14 vol% linear type CNTs, and without CNTs produced with the water based zwitterionic surfactant solution were 253, 239, and 178 MPa, respectively.

TEM observations revealed two facts that thin MgO layer was presented at the interface between CNTs and Mg matrix, and excess amount of MgO particles aligned at grain boundaries. The former was effective to the tensile loading transfer from Mg matrix to strong CNTs. However, the latter decreased elongation of the composites. To improve the composite elongation, the production of the excess amount of MgO was regulated using the IPA based solution.

Fig 1.8 shows nominal stress and nominal strain curves of the pure Mg/CNT composite fabricated via the described process. Differences in the yield stress at 0.2% offset and tensile strength between pure Mg/CNT composite and pure Mg without CNTs were insignificant. Fig. 9(a) and (b) exhibits the fractured surface of pure Mg/CNT composite. Lots of CNTs were stuck on the fractured surface of the composite with showing nearly same shape and length as they were on the composite powders [92].

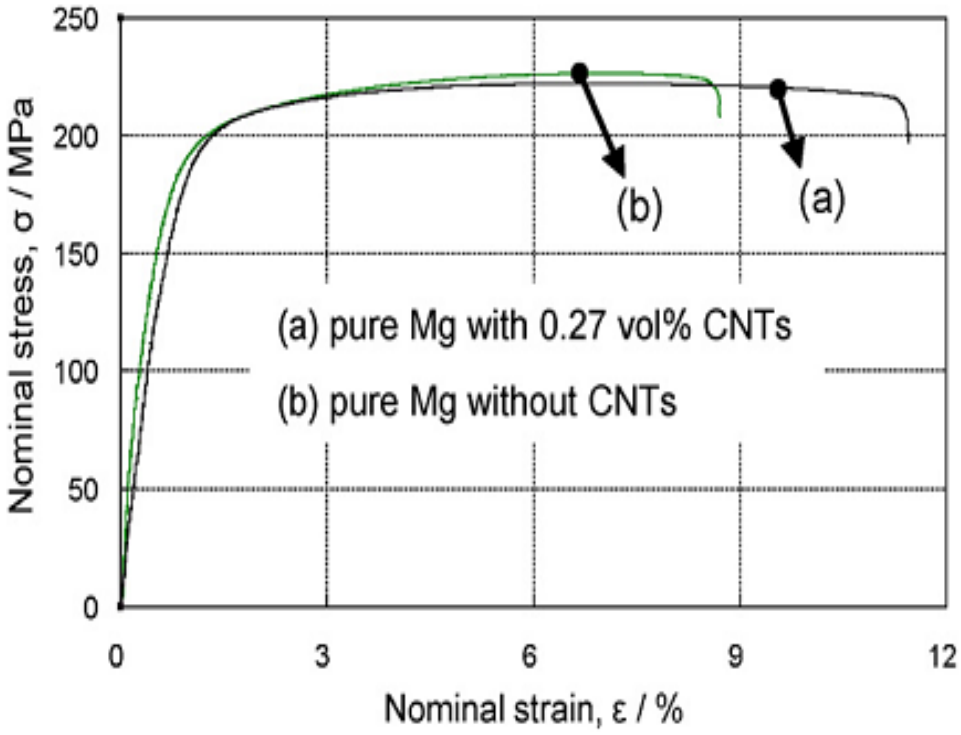

Figure 1.8. Tensile behavior of pure Mg with 0.27 vol% CNTs (a), and pure Mg without CNTs (b). By incorporating CNTs, elongation was increased though both yield stress at 0.2% offset and tensile strength were not improved [92].

Due to the poor interfacial bonding between Mg matrix and CNTs without MgO, CNTs were detached from the Mg matrix before they were damaged or fractured by the tensile loading. Though naturally formed MgO on as-received powder surface should reinforce the interface between Mg matrix and CNTs, only these MgO could not provide enough interfacial strength. lots of pull-out of carbon fibers on the fractured surface of pure Mg composite with SiO2 coated carbon fibers. They concluded that this was due to the relatively weak interfacial bonding of carbon fibers with MgO. However, in their article, the mechanical properties of the composite were apparently improved compared to that of pure Mg without carbon fibers [93].

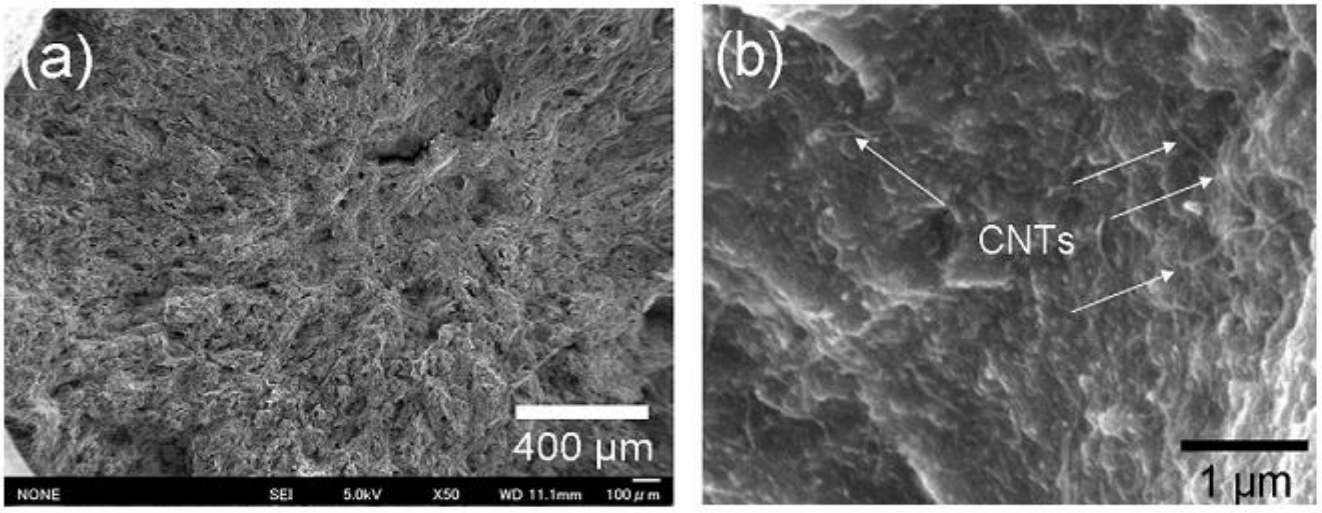

Figure 1.9. Fractured surface of pure Mg/CNT composite. (a) and (b) Are low and high magnification photos, respectively. As shown in (b), some CNTs were present on the fractured surface as they were on the composite powder surface [95].

MgO was artificially produced by SiO2 reduction and more or less strengthened the interface between Mg matrix and carbon fibers. By taking into consideration, it can be concluded that the artificial MgO production was required to obtain suitable interfacial bonding between Mg matrix and CNTs. On the other hand, elongation of pure Mg was increased by CNT addition as shown in Fig.8. Two possible reasons successfully explain this improvement; one is MgO elimination from the matrix as former described and the other is decrease of residual strain in the matrix [95]. During the hot extrusion processing, the extrusion load of sample with and without CNTs were about 483 and 563 kN, respectively.

The extrusion load was significantly decreased by the addition of CNTs. Many articles reported that CNTs could reduce friction co-efficient of the matrix materials. For example, Ni/CNTs composite coating on the carbon steel plate reduced friction co-efficient compared to those of Ni, Ni/SiC and Ni/graphite coatings [95]. In the present study, since the interfacial bonding between Mg matrix and CNTs was relatively low, some of the interfaces could be broken out during the hot extrusion process due to the severe plastic deformation [92,95]. Consequently, some free CNTs were definitely produced in the matrix. Non-damaged CNTs on fractured surface shown in Fig 1.9(b) could be regarded as one of the examples.

As CNTs serve low friction coefficient to pure Mg matrix, in situ lubrication of these free CNTs assisted the smooth deformation of the Mg matrix. Since accumulated strains in pure Mg/CNT composite were less than that of pure Mg without CNTs before tensile test, pure Mg/CNT composite could elongate higher than pure Mg without CNTs.Vickershardness values of 42.40 HV for samples with CNTs and 43.50 HV for samples without CNTs also justified the explanation above. Despite the incorporation of hard CNTs, pure Mg/CNT composite was slightly softer than pure Mg without CNTs [95].

Development of amorphous alloy/glassy particle reinforced light metal composites is an emerging research field. In this investigation, we have synthesized and characterized $Ni_{60}Nb_{40}$ amorphous alloy particle reinforced Mg-composites with varying volume fractions. Microwave-assisted two-directional rapid sintering technique followed by hot extrusion was used to produce these pure Mg-based composites. The structural and mechanical properties of the developed composites were investigated [96].

Structural analysis indicated the retention of amorphous structure of the reinforcement in all the composites. It was found that the distribution of the reinforcement was strongly dependent on the volume fraction (Vf). The addition of $Ni_{60}Nb_{40}$ amorphous alloy particles modified the preferred crystal orientation of Mg, as was observed from X-ray diffraction (XRD) analysis. The composites showed significant improvement in hardness (increment up to 120%) and compressive strength (85% increase at 5% Vf). Comparison of mechanical properties of the developed composites with those of conventional Mg-composites having ceramic/metallic reinforcements, highlight the effectiveness of using amorphous particles as promising reinforcement materials.

Amorphous alloys/bulk metallic glasses (BMG) are a new class of metallic materials that are different from conventional crystalline metals/alloys. These materials do not have long-range atomic order, unlike crystalline materials. They are metastable in nature, and exhibit glass transition (Tg) and crystallization (Tx) temperatures. Due to their unique structure, amorphous alloys/BMG possess extremely high strength (>1 GPa), large elastic strain limit of 2% (conventional crystalline metals have elastic strain limit of 0.2%) and superior corrosion resistance.

Looking at the unique properties of the amorphous alloys/BMG, it is advantageous to use them as reinforcements for making light metal composites. On the incorporation of amorphous alloys/BMG as reinforcements in metal matrices are in the early stages. [37,38] fabricated Al-MMCs reinforced with Ni–Nb– Ta amorphous alloy ribbons by squeeze infiltration technique and observed 25% improvement in compressive strength. used Zr- and Ni-base glassy particles as reinforcements in metallic matrices via powder metallurgy technique and observed 60–90% enhancement in compressive strength.

Improvements in compressive strength were also observed in Zr-, Cu- and Fe-based glassy ribbons reinforced Mg and Al-matrices produced using powder metallurgy-based hot compaction by induction heating method. In the class of powder metallurgy (PM) based techniques, the microwave assisted rapid sintering process is energy conservative and can efficiently produce light-metal composites. This technique employs two-directional heating to sinter powder compacts, through a combined action of microwaves and microwave-coupled external heating source. By this process, sintering temperatures even close to the melting point of light metals such as Al, Mg can be achieved, in a relatively shorter period of time, resulting in a dense product with negligible porosity [96].

Magnesium-based materials have shown the potential to serve as biodegradable metal implant suitable for repair of load-bearing defects in osseous tissue. However, the mechanical properties of magnesium alloys were low for the load-bearing applications, and the corrosion resistance also needed to be improved furthermore. Design and preparing of a nanocomposite based on magnesium alloy might be an approach to this challenge. The effect of Fluor apatite (FA) Nano-particles content on microstructure, mechanical properties and bio-corrosion behavior of a nanocomposite (AZ91-FA) made of AZ91 magnesium alloy as matrix and FA Nano-particles as

reinforcement for load-bearing applications. Novel AZ91-FA (with 10 wt.%, 20 wt.%, and 30 wt.% of FA) nanocomposites were produced by AZ91 magnesium alloy powders and FA Nano-particles using a blend press-sinter powder metallurgy (PM) method. Microstructure, mechanical properties and bio-corrosion behavior of the prepared AZ91-FA nanocomposites, and also the AZ91 magnesium alloy as control sample.

The results showed that the presence of the FA Nano-particles in the AZ91 magnesium alloy matrix led to significant improvement in hardness and elastic modulus. The AZ91-FA nanocomposite with 20 wt.% of the FA Nano-particles showed the highest yield strength, and with the increase of the FA content in the AZ91-FA nanocomposites, the ductility decreased. The AZ91-FA nanocomposites presented increased corrosion resistance compared to the AZ91 magnesium alloy and the corrosion resistance of the AZ91-FA nanocomposites increased with an increase in FA content. The AZ91-FA nanocomposite with 20 wt.% of the FA Nano-particles showed optimum mechanical properties as well as the corrosion resistance [36,97].

Stress–strain curves for the AZ91 magnesium alloy and AZ91- FA nanocomposites are shown in Fig 1.10 and their compressive properties and densities are summarized in Table 3.1 The compressive yield strength for the AZ91-FA nanocomposites increased with an increase in the content of the FA Nano-particles added, and they reached maximum values when 20 wt.% of the FA nanoparticles were added.

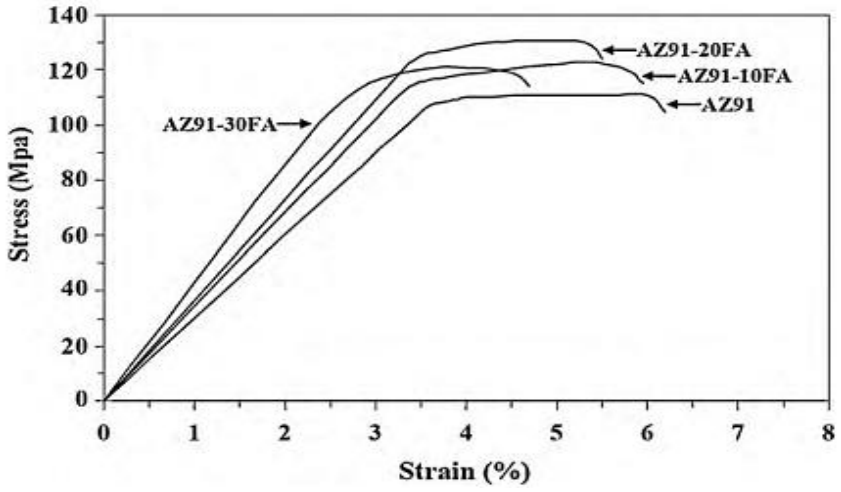

Figure 1.10. Compressive stress–strain curves for AZ91 magnesium alloy and AZ91 FA nanocomposites [97].

In general, the yield strength is the stress required to operate dislocation sources and is governed by the presence and magnitude of all the obstacles that restrict the motion of dislocations in the matrix. Under applied compressive stress, multi-glide planes agglomerate to form grain boundary ledges and these ledges act as obstacles to dislocation movement resulting in pile-ups, causing the significant increase in the yield strength of the composites over magnesium.

Unfortunately, when the addition of the FA nanoparticles is greater than 20 wt.%, the deterioration in yield strength can be explained by the enhanced agglomeration of the FA nanoparticles and thereby the formation of pores and defects [98]. The results of elastic modulus measurements revealed that an increase in the weight percentage of the FA Nano-particles led to an increase in the elastic modulus (see Table 3.1). Increase in the elastic modulus of the AZ91 magnesium alloy matrix can be attributed to the presence of: (a) high elastic modulus of reinforcement, and (b) uniform distribution of reinforcement with good interfacial integrity.

Table 2.2 Compressive properties and densities of AZ91 magnesium alloy and AZ91-FA nanocomposites [98].

Materials	Microhardness (HV)	Elastic modulus, E (GPa)	Compressive yeild strength, σ_Y (MPa)	Ductility, ε (%)	Density ρ (g/cm^3)
AZ91	80	30.2	105.3	6.15	92.7
AZ91•10FA	86	34.1	116.5	5.78	94.1
AZ91•20FA	93	37.5	123.2	5.32	95.8
AZ91•30FA	105	42.3	112.4	4.51	93.2

It may be noted that the uniform distribution of reinforcement coupled with the good matrix–reinforcement interfacial integrity led to a significant increase in internal stress between reinforcement and matrix resulting in the enhancement of elastic modulus. Ductility of the AZ91 magnesium alloy matrix is about 6.15%while the ductility of all the three AZ91-FA nanocomposites decreases with an increase in the FA Nano-particles contents reinforcements (see Table 3.1). For powder metallurgical processed composites, reinforcement particles are usually located along interfaces of matrix particles [37].

The presence of hard particles along interfaces may limit deformation of matrix particles caused by dislocation movement together with twining. Effectiveness of restriction to deformation of particles is dependent on the amount of reinforcement as well as the interfacial bonding between matrix and reinforcement particles. Although higher content of reinforcement may promote strengthening, agglomeration of the reinforcement particles may degrade the ductility effect, and even may introduce micro voids between them [97].

2.6 Reinforced magnesium based composites chemical reactivity

Mg/Ca (1 wt.%, 5 wt.%, 10 wt.% Ca) composites were prepared from pure magnesium and calcium powders using the powder metallurgy method, aiming to enlarge the addition of Ca content without the formation of Mg_2Ca. The microstructures, mechanical properties and cytotoxicity's of Mg/Ca composite samples were investigated. The corrosion of Mg/Ca composites in Dulbecco's modified Eagle's medium (DMEM) for various immersion intervals was studied by electrochemical impedance spectroscopy measurements and environmental scanning electron microscope, with the concentrations of released Mg and Ca ions in DMEM for various immersion time intervals being measured. It was shown that the main constitutional phases were Mg and Ca, which were uniformly distributed in the Mg matrix [98].

The ultimate tensile strength (UTS) and elongation of experimental composites decreased with increasing Ca content, and the UTS of Mg/1Ca composite was comparable with that of as-extruded Mg–1Ca alloy. The corrosion potential increased with increasing Ca content, whereas the current density and the impedance decreased. It was found that the protective surface film formed quickly at the initial immersion stage. With increasing immersion time, the surface film became compact, and the corrosion rate of Mg/Ca composites slowed down. The surface film consisted mainly of $CaCO_3$, $MgCO_3$ $3H_2O$, HA and $Mg(OH)_2$ after 72 h immersion in DMEM. Mg/1Ca and Mg/5Ca composite extracts had no significant toxicity ($p > 0.05$) to L-929 cells, whereas Mg/10Ca composite extract induced 40% reduced cell viability [99].

Fig.1.11 shows the OCP–time curves for Mg/Ca composites with different Ca contents during 40,000-s immersion in DMEM. At first, the potentials of the Mg/1Ca, Mg/5Ca and Mg/10Ca composite samples increase rapidly, resulting from the precipitation of the protective surface films. Subsequently, a sharp drop in the potential occurs at 2000 s for Mg/1Ca composite, indicating the

occurrence of pitting corrosion, and the corrosion potential experiences a short anodic polarization thereafter. Mg/5Ca composite exhibits a similar OCP curve to Mg/1Ca composite, and the drop in the potential can be seen at 1000 s. For the Mg/10Ca composite sample, only a tiny drop in potential occurs at 5500 s, and intensive fluctuation in the corrosion potential appears during subsequent immersion [100].

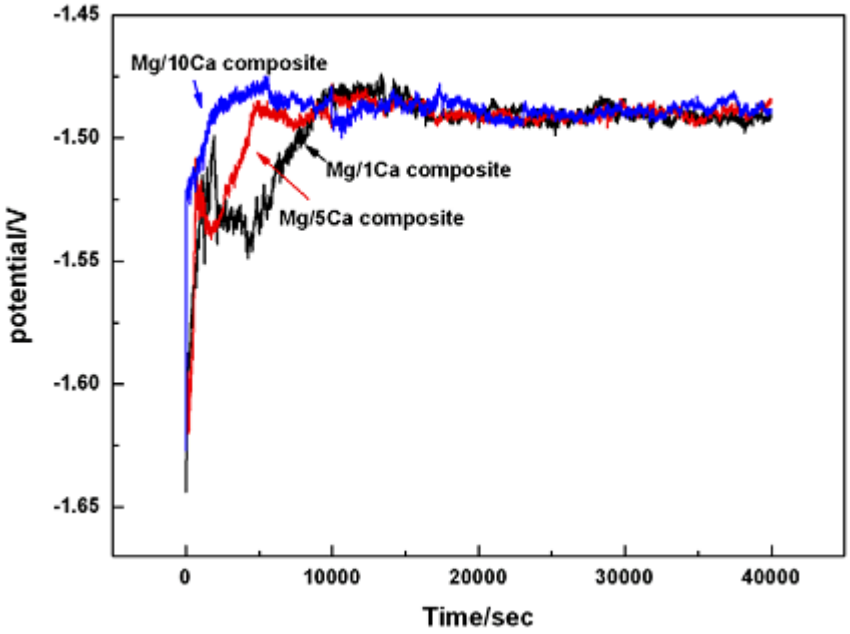

Figure 1.11 OCP curves of Mg/1Ca, Mg/5Ca and Mg/10Ca composite samples in DMEM [100].

In addition, it can be seen that the corrosion potential of the three Mg/Ca composite samples increases with increasing Ca content in the first 10,000 s immersion. This may be attributed to the different Ca contents for different Mg/Ca composite samples. For example, the larger amount of Ca ions released for the Mg/10Ca composite sample may cause CaCO3 precipitation on the surface of the samples, which can provide a better protective effect, together with Mg(OH)2, against pitting corrosion than a simple Mg(OH)2 surface film can [101].

The corrosion potentials for the three samples exhibit a similar fluctuating tendency in the potential range (1.5 V vs SCE and 1.47 V vs SCE) after 10,000 s immersion, which reveals further spreading of the existing corrosion pits and/or formation of new pits.

Fig.1.12 shows the potentiodynamic polarization curves obtained for the Mg/Ca composites with OCP measurements taken after immersion in DMEM for 40,000 s. It can be seen that the corrosion potential increases in the order of E_{corr}(Mg/1Ca) < E_{corr} (Mg/ 5Ca) < E_{corr}(Mg/10Ca) [101].

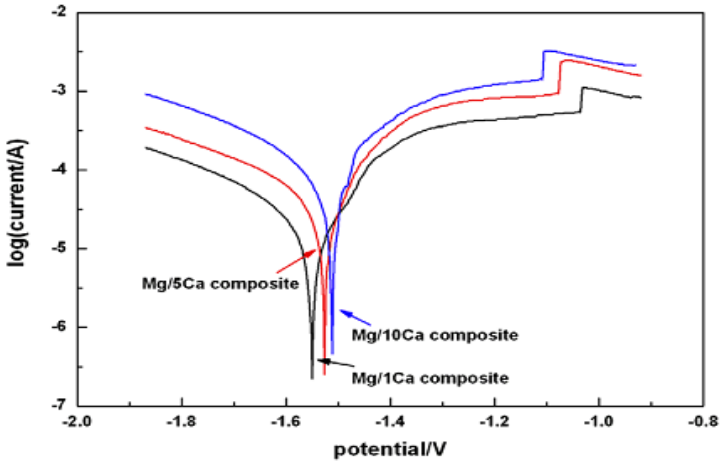

Figure 1.1 Potentiodynamic polarization curves of Mg/1Ca, Mg/5Ca and Mg/10Ca composite samples in DMEM [101].

The cathodic polarization current shows that the hydrogen evolution reaction on Mg/1Ca composite samples (the current density is 46.24 μA Cm^{-2}, at 1.65 V) is much lower than that on the Mg/5Ca (102.3 μA Cm^{-2}, at 1.65 V) and Mg/10Ca composite samples (254 μA Cm^{-2}, at 1.65 V) [101].

In this study, Mg composites are reinforced with biocompatible tantalum (Ta) and Hydroxyapatite particles through the PM process will be synthesized. Because of their surface oxide layer's stability tantalum are highly corrosion resistant. Corrosion resistance generally correlates with biocompatibility (although not always), because more stable metal oxides tend to be less chemically active and/or biologically available and are thus less participatory in biologic processes. The effect of biocompatible Ta and Hydroxyapatite particulates on the microstructure, morphology and mechanical properties of Mg matrix are investigated. Moreover, the mechanical properties of composite materials are examined via micro hardness and compression test and also the morphology and intermetallic phase was examined by Scanning Electron Microscope and XRD respectively. The optimal parameters to fabricate Mg composites via powder metallurgy process are recommended.

CHAPTER THREE

3. MATERIALS AND METDOLOGY

- Commercially available
    1. Mg powders (99% purity, 60≤ size ≤220 µm,)
    2. Ta powders (99.99% purity, 2≤ size ≤35 µm, Sigma-Aldrich USA) and
    3. Hydroxyapatite (Reagent level, Sigma-Aldrich south Korea) were used as starting materials.

Figure 2.1 Raw materials and balance

- Mixture of Mg-Ta-HA powders at a nominated ratio of Mg and Ta and HA powders were prepared by high energy ball milling.

Table 3.1 Composition and Fraction of Reinforcement in wt.%.

Composition	Fraction of Reinforcement wt%		
	Mg	Ta	HA
Mg	100	0	0
Mg3Ta7HA	90	3	8
Mg6Ta7HA	87	6	8
Mg9Ta7HA	84	9	8

- The ball milling was performed with a planetary ball mill PM 400-Retsch for 9 h. The ball-to-powder ratio was 20:1 and ball milling was carried out at rotation speed of 200 rpm.
- The milled pure Mg powder, as control material, and homogeneous Mixture of Mg-Ta-HA powders were uniaxial pressed at a pressure of 70 MPa into cylindrical compact.

Figure 2.2 Compacted green body at different composition

- The green compacts were then sintered at 550 ℃ for 3 hours under inert atmosphere by Tube furnace.

Figure 2.3 Tube Furnace

Figure 2.4 Sintered samples at different wt% reinforcement

- The density of pure Mg and composites was measured using the Archimedes' Principle. Three randomly selected samples were weighted in air and distilled water, using an electronic balance, with an accuracy of ± 0.0001g.

Figure 2.5 Measuring of the density of the composite.

- By using rule of mixture (ROM) we can calculate theoretical density of each composition.

$$\rho_{composite} = \rho_{matrix} * V_{matrix} + \rho_{reinforcement} * V_{reinforcement}$$

- By using $Archimedes$ principle we can calculate experimental density and porosity.

$$Archimedes\ density = \frac{weight\ of\ sample\ in\ air}{weight\ of\ sample\ in\ air - weight\ of\ sample\ in\ water}$$

$$Archimedes\ percent\ porosity = \frac{wet\ weight - dry\ weight}{wet\ weight - weight\ of\ sample\ in\ water}$$

- ❖ The sintered samples were then grounded, using 1200 grit SiC paper, and micro-hardness test was carried out using Highwood HWDV-7S micro hardness tester accordance with ASTM E384-99 standard.
- ❖ The x-ray powder diffraction (XRD) was performed on an Analytical X-pert Powder diffractometer (Netherlands) with CuKα radiation.
- ❖ Finally, Instron universal tester (Instron 5567, 30 kN,) was used for compression test of cylindrical samples with a size of Φ20×9 mm^2 with an initial strain rate of 10^{-3} s^{-1}. A total of 6 samples were tested for each composition.

Figure 2.6 Compressed samples of pure Mg, Mg-Ta-Ha composites after compression test.

CHAPTER FOUR

4. RESULT AND DISCUSSION

As can be seen in Fig. 3.1, Mg-Ta-HA composites were fabricated successfully through powder metallurgy process. Pure Mg was also fabricated as a reference material. Table 4.1 represents the density and porosity of current pure Mg and Mg composites. Rule-of-mixture (ROM) approach (Eq. (1)), based on the values of density (ρMg=1. 739gm/cm^3, ρTa = 16. 69 gm/cm^3,ρHA =3.15 gm/cm^3) and volume fraction of metal matrix and reinforcements, was used to calculate the theoretical density of composite materials [102–104].

$$\rho_{composite} = \rho_{matrix} \text{ X } V_{matrix} + \rho_{reinforcement} \text{ X } V_{reinforcement}$$

Where, ρ is density (gm/cm^3) and V is volume fraction (vol%).

Table 4.1 porosity and density of pure Mg and Mg-Ta-HA composites

Composition	Fraction of reinforcement				Density (gm/cm^3)		Porosity (%)
	Ta (Wt%)	HA (Wt%)	Ta (Vol%)	HA (Vol%)	Theoretical	Experimental	
Mg	0	0	0	0	1.74	1.7474± 0.005	2.5
Mg3Ta8HA	3	8	3.3	4.7	1.77	1.7602 ± 0.001	2.6
Mg6Ta8HA	6	8	6.9	4.85	1.82	1.7803± 0.001	2.45
Mg9Ta8HA	9	8	10.6	5.0	1.91	1.8484± 0.002	2.36

The low differences between theoretical and experimental densities approve the feasibility of fabrication of almost dense pure Mg and Mg composites through PM and milling processes.

Figure 3.1 Sintered pure Mg and Mg-Ta-HA composites fabricated through powder metallurgy process.

During the powder pressing the compaction pressure is typically 70MPa and the metal particles will rearrange with the pressure exerted by the punches and interlocking between them occurs due to their irregular shape. Sometimes even cold welding of the particles can take place at high pressures. This gives the compact sufficient green strength.

However, micro-pores are observed in the microstructures. The presence of porosity is due to the trapped air between Mg particles which is related to the fabrication method i.e. it is the normal characteristic of powder metallurgy process. It also could be related to the volume shrinkage of Mg powders [105]. the presence of the pores in the PM steels will have an unprecedented effect on the material properties as they result in stress concentration regions. Still, the major issue with PM steel is of course the pore characteristics.

The measurement of the average particle size of Mg powders (Fig. 3.2) also shows that the average size of Mg powders is reduced due to mechanical milling. The average particle size of Mg powders is reduced by addition of reinforcement materials in the mixture powders. In Mg-Ta-HA mixtures, the addition of 3, 6 and 9 wt% Ta and 8 wt% HA to Mg powder through milling process decreases the average size of Mg powders from ~130 µm to ~76, ~68 and ~60 µm, respectively; while in by increase of Ta content to 3, 6 and 9 wt%, respectively.

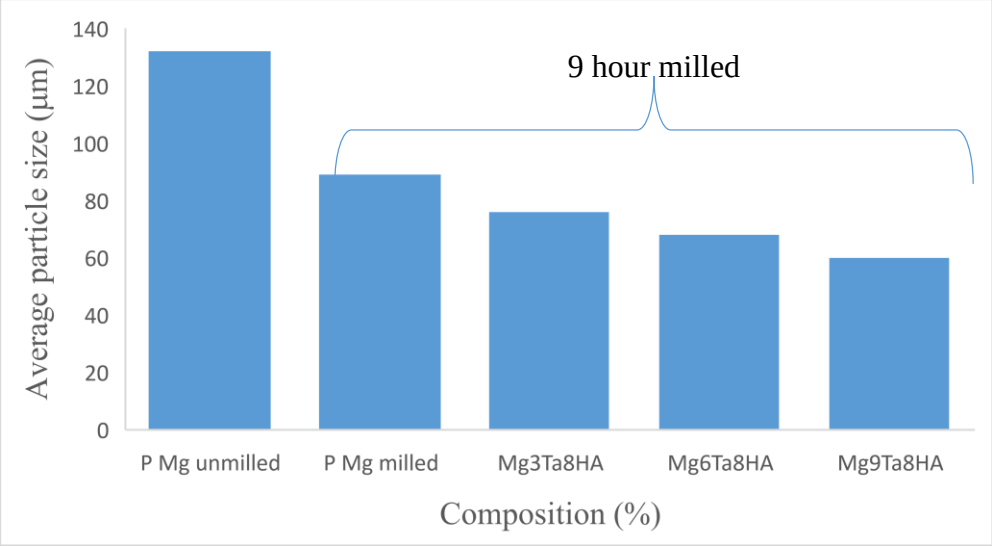

Figure 3.2 Average particle size of pure Mg unmilled, milled Mg and milled Mg composites for 9 hours.

The reduction in size of Mg powders in mixtures through milling process can be attributed to the friction of Mg powders by reinforcement materials. In such case, reinforcements act like abrasive materials due to higher hardness of HA (115–160 HV) and Ta particles (90–200 HV) than that of Mg (30–45 HV) [69,70]. Therefore, the compressibility of the green compacts and attachment of particles during sintering process are improved, indicating higher densification and less porosity in the samples [106].

In the first stage of sintering, the powder is compacted; the particles are in contact with one another, but are not physically bonded in any way. The compacted powder is heated to a temperature that is generally about 2/3 of *T*m, the melting point. At this stage, "necks" begin to form between the particles, bonding them together.

The small contact areas between the particles expand, and at the same time, the density of the compact increases, as well as the total void volume decreases as we see in (fig. 3.3a and fig. 3.3b) respectively. Small diameter particles will have a high surface area and a high surface free energy.

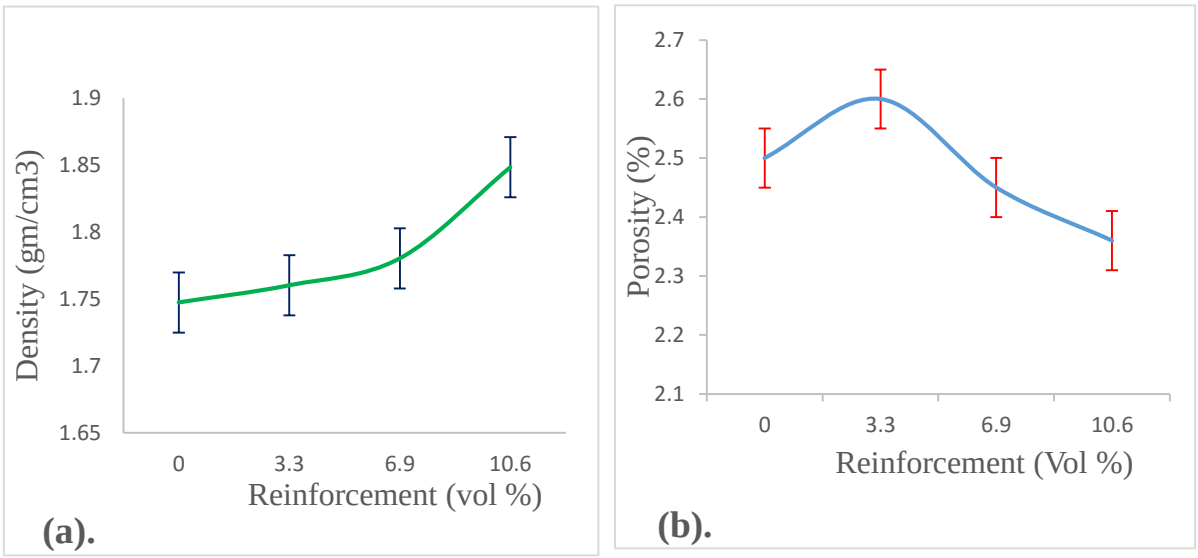

Figure 3.3 (a). Density and (b). porosity of pure Mg and Mg composites.

The high surface free energy of the particles is the driving force of the sintering process. Therefore, there is a strong thermodynamic drive to decrease the surface area by bonding particles together. As the number of bonds grows, the surface area and, thus, energy are reduced.

In the final stage of sintering, individual particles can no longer be seen, as they are fully bonded together, leaving residual porosity in the form of closed-off pores that are of a sufficiently small diameter, so as not to have the original powder particle size will control the final pore size and distribution: the smaller the particle size, the smaller the pores and the better the mechanical properties will be.

And also, the mechanical properties are affected by the amount of pores, their size distribution and pore morphology. Depending on the kind of pores there are differences in their impact. Open or interconnected pores have more significant effect on mechanical properties rather than isolated and closed pores. However, the porosity in current samples is agree with and even better than other PM-processed Mg composites [107].

In addition, high pressure and sintering temperature used to consolidate Mg powders to green compact and attach particles together, respectively. Thus, low enclosed air was entrapped between powders, resulted in low porosity in the microstructures and also reduced size of Mg powders, achieved through mechanical milling, can reduce the porosity in the samples.

The uniform distribution of HA and Ta particles in Mg matrix and The nearly zero standard deviation of measured densities (Table 4.1) also supports the uniform distribution of such reinforcements in Mg composites.

In this study, closely positioned particles were observed by addition of reinforcement. High-particle concentrated areas -originated from large difference in density between Mg, Ta and HA (1.74, 16.69 , 3.15 gm/cm^3, respectively [108])- are not observed. And also, the ultrafine HA and Ta particles uniformly distribute in the Mg matrices with small porosity for the composites containing 3, 6 wt.% Ta. For the composites containing 8 wt.% HA, however, HA particles agglomerate in the Mg matrices, and some obvious voids appear at Mg3Ta8Ha composite then the distribution of voids will be decreased due to the increased wt% of Ta. Moreover, agglomeration of HA particles in the composites is enhanced with addition of HA from 7.5 to 10 wt.%.

The reasonably uniform distribution of Ta particles for the 3,6 wt % Ta composites can be attributed to suitable mixing parameters. However, a limited amount of clustering of reinforcement was unavoidable in high content of HA and Ta, owing to the high surface energy associated with the ultrafine particles [109].

The low difference between theoretical and experimental density of reinforcement particles revealed a defect-free interface due to uniform distribution of reinforcements particles on Mg matrix. This fact, despite of high difference in melting point of Ta (3017 ℃) or HA (1250 ℃) with Mg matrix (650 ℃) [108,110] and limited solid solubility of HA or Ta in Mg [111,112] approves that proper bonding of reinforcements with Mg matrix can be achieved through milling and sintering processes.

Fig. 3.4 presents the XRD results of the Mg composites. In addition to the peaks attributed to Mg, there are distinguishable Ta and HA peaks in the XRD patterns. It is shown that the Ta peaks are stronger in 9 wt.% Ta-containing composite than those in 3 wt.% or 6 wt.% Ta-containing composite. No peak relating to new intermetallic compounds between Mg and reinforcements can be detected. This confirms no reaction occurs between Mg and reinforcement particles and supports the formation of Mg composite structures.

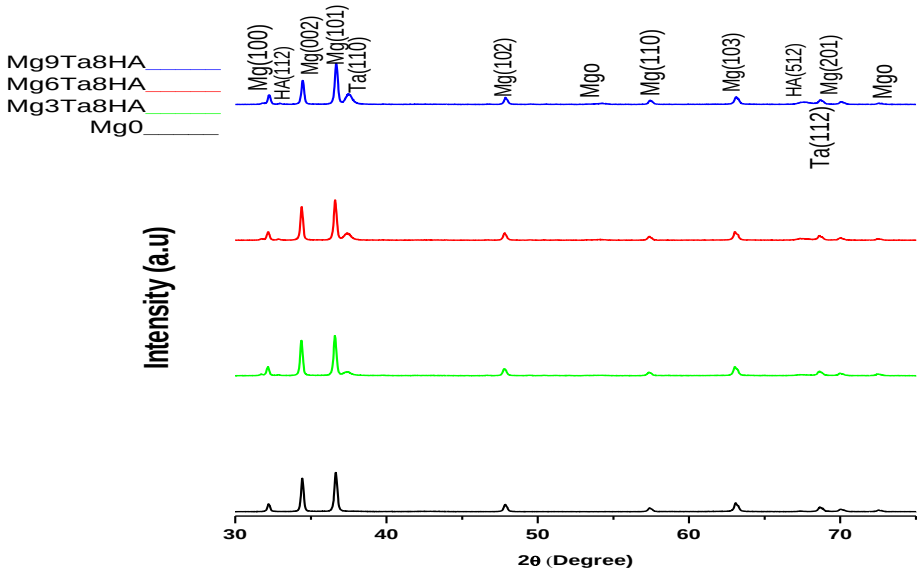

Figure 3.4 X-ray diffraction pattern of Mg composites

Based on the report that intermetallic phases could cause embrittlement and weaken the interfacial bonding of particle/matrix and in turn affect the mechanical properties of the composites [113], it is expected that no existence of reactive product between Ta, HA and Mg can improve the properties of Mg-Ta-HA composites and also when the tantalum volume fraction increase the intensity was decreased due to smaller particle size and lattice strains so, it increases the mechanical properties of the composites.

Fig 3.5 shows the microhardness values of pure Mg and the Mg composites. The hardness values increase significantly with increasing V_f of Ta and HA , such that at 10.6%V_f, increase in hardness value up to 190% is observed, when compared to pure Mg. The increase in microhardness values is due to the high hardness of the Ta and HA reinforcement particles (measured in the present work to be Ta (90–200 HV) and HA (90–200 HV)). Such high hardness of the reinforcement particle would increase the matrix work-hardening, thereby resulting in higher hardness of the composites. And also, this increment can be ascribed to addition of harder reinforcement materials to Mg matrix which restricts the local deformation of matrix during the indentation process shown in (fig. 3.6).

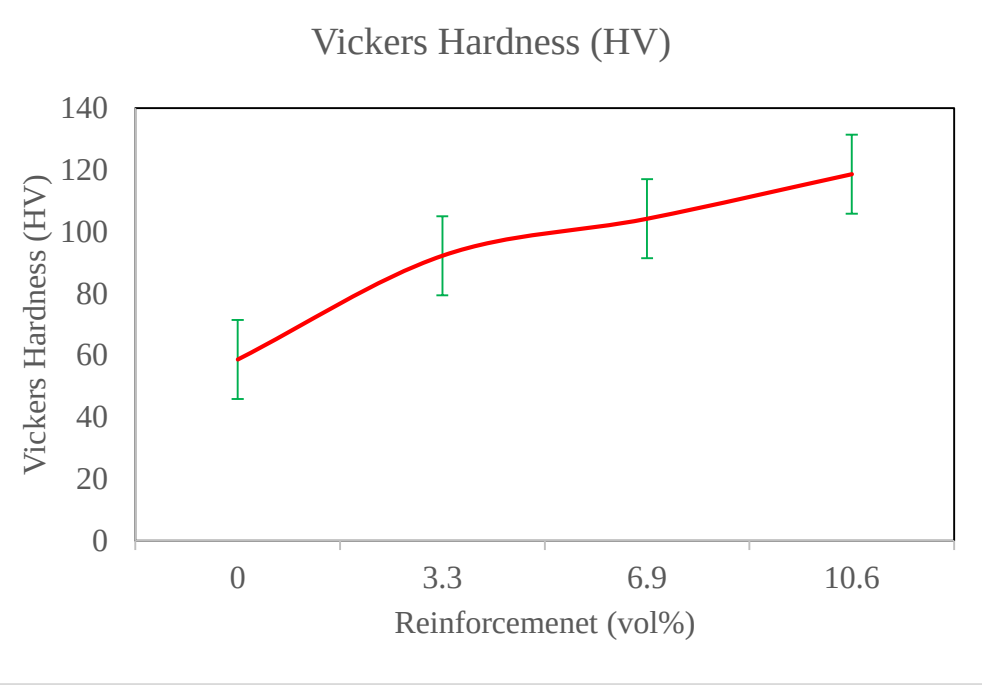

Figure 3.5 Microhardness of pure Mg and Mg-Ta-HA composites.

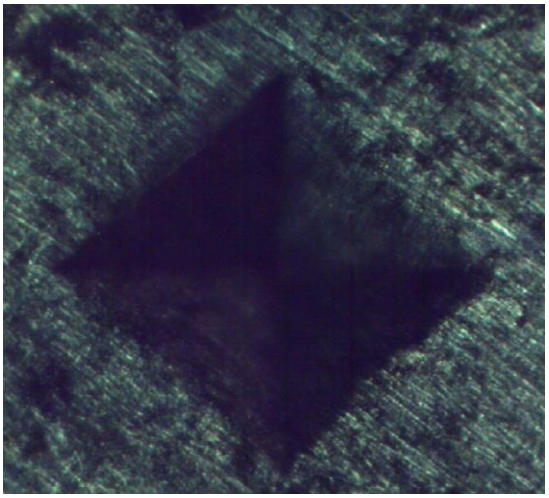

(a).

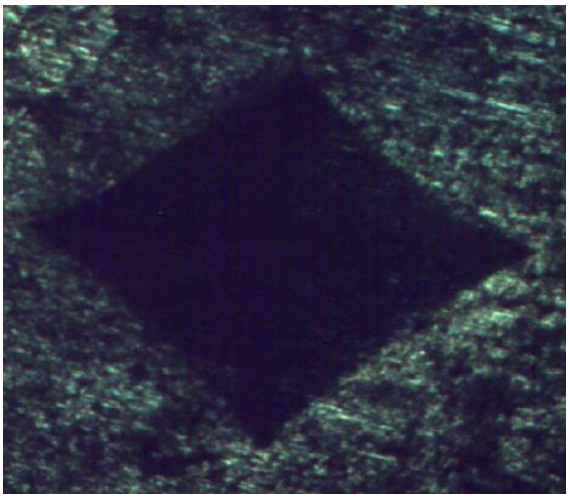

(b).

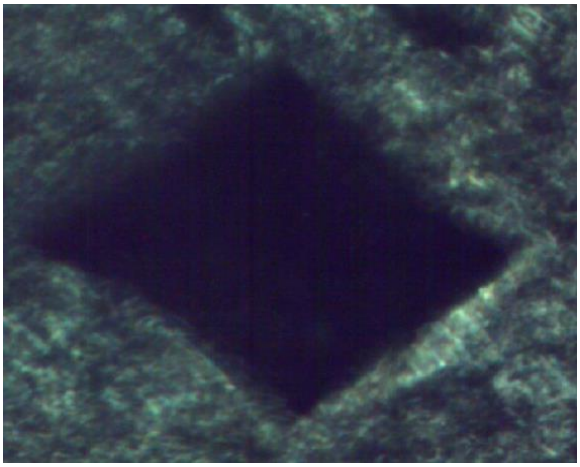

(c).

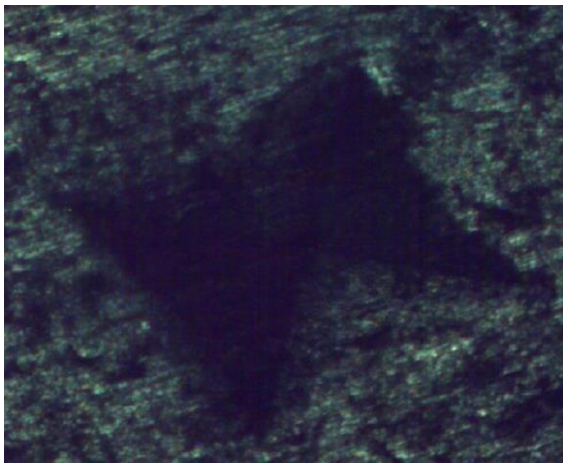

(d).

Figure 3.6 Vickers hardness Indentation images of (a). pure Mg (b). Mg3Ta8HA (c). Mg6Ta8HA (d). Mg9Ta8HA composites.

The significant enhancement in microhardness values obtained in the developed composites are found to be superior/on part with those of the conventional metallic/metallic particle reinforced composites. This shows that the high elastic strain of the amorphous reinforcement particles plays an important role in the retention/increase in the ductility of the composites.

The compressive stress-strain curves and compressive properties of pure Mg and Mg composites are shown in Fig. 3.7 Engineering stress σ is defined by the relationship

$$\sigma = \frac{F}{Ao}$$

Engineering strain ε is defined according to

$$\varepsilon = \frac{li - lo}{lo} = \frac{\Delta l}{lo}$$

And young's modulus

$$\sigma = E\varepsilon$$

It is therefore desirable to know the stress level at which plastic deformation begins or where the phenomenon of yielding occurs. the point of yielding may be determined as the initial departure from linearity of the stress–strain curve; this is sometimes called the proportional limit, and represents the onset of plastic deformation on a microscopic level. The position of this proportional limit is difficult to measure precisely. As a consequence, a convention has been established by which a straight line is constructed parallel to the elastic portion of the stress–strain curve at some specified strain offset, usually 0.002 as we see in fig 25. The stress corresponding to the intersection of this line and the stress–strain curve as it bends over in the plastic region is defined as the yield strength.

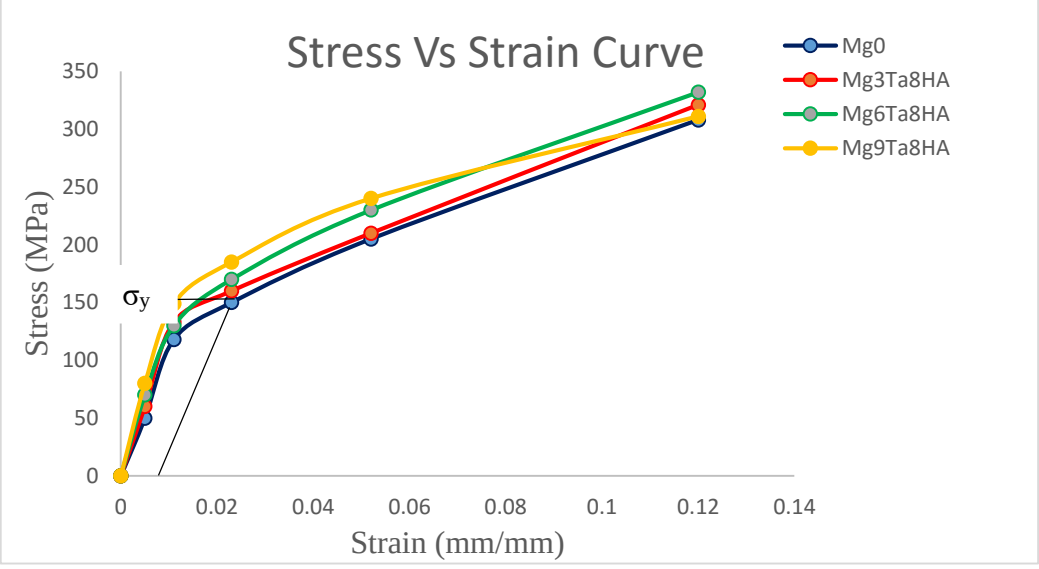

Figure 3.7 Stress –strain curve of Pure Mg and Mg-Ta-HA composites.

The compressive yield strength for the Mg-Ta-HA composites increased with an increase in the content of the Ta particles added, and they reached maximum values when 9 wt.% of the Ta particles were added as shown in (fig.3.8). The compressive properties were greatly improved by introducing a small content of the Ta particles could be explained by the homogeneous distribution of the Ta and HA particles in the vicinity of the magnesium matrix grain boundaries; because the Ta particles were believed to impinge on the near surface of the magnesium powders very homogeneously during a mixing process [114].

The yield strength is the stress required to operate dislocation sources and is governed by the presence and magnitude of all the obstacles that restrict the motion of dislocations in the matrix. Under applied compressive stress, multi-glide planes agglomerate to form grain boundary ledges and these ledges act as obstacles to dislocation movement resulting in pile-ups, causing the significant increase in the yield strength of the composites over magnesium [115].

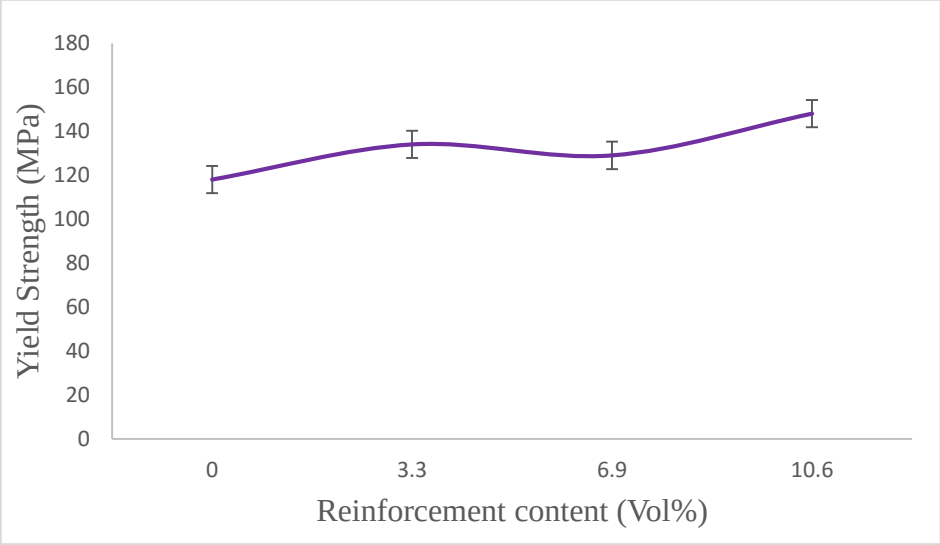

Figure 3.8 Yield strength of pure Mg and Mg composites obtained from stress-strain curve.

In metal matrix composites, the differences in thermal expansion coefficients of the matrix and the reinforcements would result in the introduction of thermal residual stress in the composite [116]. The presence of thermal residual stresses would increase the dislocation density at the particle/matrix interface and hence would contribute to the improvement in the yield strength of the composites.

Unfortunately, when the addition of the Ta particles is 6.9 Vol% as shown (fig. 26), the deterioration in yield strength can be explained by the enhanced agglomeration of the Ta particles and thereby the formation of pores and defects [115].

The results of elastic modulus revealed that an increase in the weight percentage of the TA particles led to an increase in the elastic modulus. The highest increase in elastic modulus (Fig. 3.9) in Mg-Ta-HA composites can be observed when the content of reinforcements is 10.9 vol% of Ta. Increase in the elastic modulus of the magnesium matrix can be attributed to the presence of:

(a) high elastic modulus of reinforcement [114], and

(b) uniform distribution of reinforcement with good interfacial integrity [115].

It may be noted that the uniform distribution of reinforcement coupled with the good matrix–reinforcement interfacial integrity led to a significant increase in internal stress between reinforcement and matrix resulting in the enhancement of elastic modulus [115]. For powder metallurgical processed composites, reinforcement particles are usually located along interfaces of matrix particles. The presence of hard particles along interfaces may limit deformation of matrix particles caused by dislocation movement together with twining.

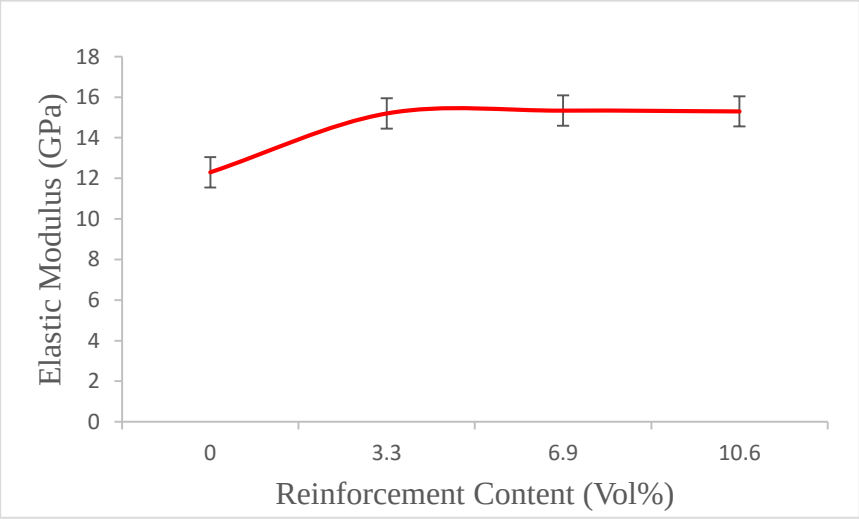

Figure 3.9 Elastic Modulus of pure Mg and Mg composites obtained from stress-strain curve.

Effectiveness of restriction to deformation of particles is dependent on the amount of reinforcement as well as the interfacial bonding between matrix and reinforcement particles.

As shown in fig.3.10 when the reinforcement content increased from 3.3 vol% to 10.6 vol% the elastic modulus was decreased. Because higher content of reinforcement may promote strengthening, agglomeration of the reinforcement particles may degrade the ductility effect, and even may introduce micro voids between them [117].

As shown in Fig. 28, the ultimate compression strengths (UCS) of the composites tend to increase when the Ta contents increase from 0 to 6.9 Vol% however, appear to decrease with the further increase of Ta from 6.9 to 10.6 Vol.%. The maximum UCS obtained from the 6.9 Vol% Ta containing composite, are about 328 MPa, higher than those of Mg by 10.6 Vol%.

A mild agglomeration of Ta particles in 10.6 Vol% Ta composites; however, the size and number of agglomerates is higher in the former composites than the latter. The results reveal that mild agglomeration does not influence the strength of the composites. In 10.6 Vol% Ta-containing composites also agglomeration of Ta particles is occurred in which the elastic properties of composites are reduced.

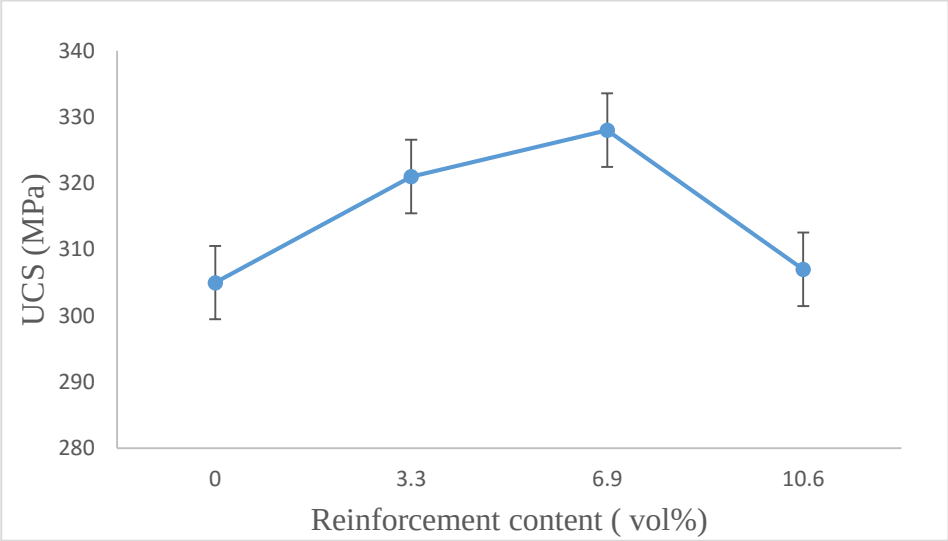

Figure 3.10 UCS of pure Mg and Mg composites obtained from stress-strain curve.

The agglomeration of reinforcement particles is mainly due to the cold welding of reinforcements during milling process. The cold welding and agglomeration of ductile particles during mechanical milling process has been reported by researchers [106,118,119].

The agglomeration of particles reduces the uniformity of distribution of the reinforcements in Mg matrix, leading to reduction of mechanical properties [120,121].

The failure strain drop can be attributed to the agglomeration of particles in Mg matrix particularly in high reinforcement-content composites. Fig.3.11 shows the Failure strain drop with the increase of Ta reinforcement content. The smaller size of Ta particulates leads to lower failure strain in Mg-Ta-HA composites. Ta particles (fine reinforcements) surround Mg powders more extremely and form a network of hard particles which bear part of applied pressure elastically. This reduces the effective compressive pressure applied to compact the powders, leading to green compacts with lower Failure strain at 10.6 Vol% Ta reinforcement content.

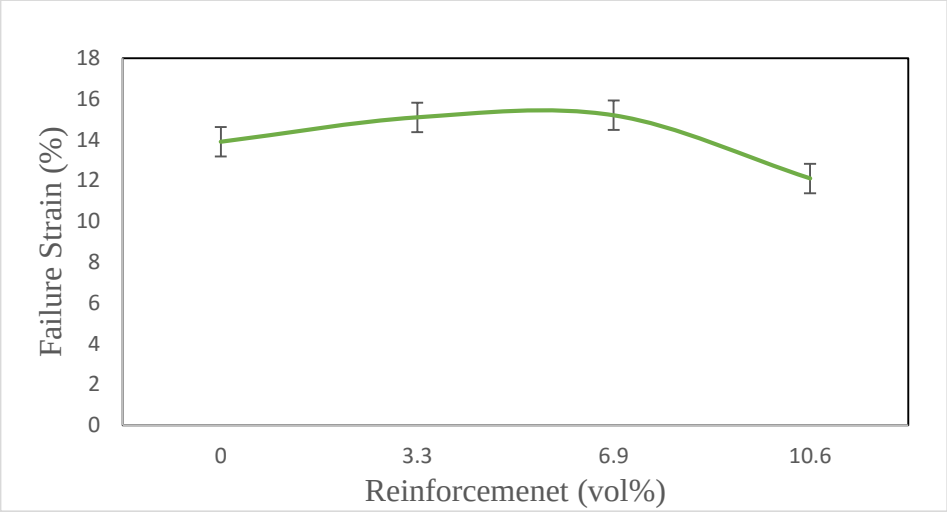

Figure 3.11 Failure Strain (%) of pure Mg and Mg composites obtained from stress-strain curve.

The increase in strengths of the composites can be attributed to the combined effects of the following factors:

(a). Orowan strengthening, e.g., owing to the presence of the dispersed small-size particles in the matrix, dislocation loops form as dislocation lines bow and bypass the particles [74];

(b). Good interfacial bonding between the Ta, HA particles and the Mg matrix gives rise to effective load transfer from matrix to Ta and HA particles which have larger load-bearing capacity [72,74];

(c). Formation of internal thermal stress due to large difference in coefficient of thermal expansion between the matrix and Ta and HA particles [72];

(d). Work hardening due to strain misfit between the reinforcing particles and matrix [74];

(e). Sphere-shaped reinforcements that have the effect of reducing interparticle spacing and the large surface area of micron-size Ta and HA particles that have the capability of generating more dislocations [73,74];

Moreover, a large number of reinforcing Ta particles act as obstacles to the dislocation movement and end up with dislocation pile ups [109,122–124]. based on the contributions by the above-mentioned strengthening mechanisms, the strengths of the composites should increase invariably with increasing weight fraction of Ta particles.

However, the strengths of the composites tend to decrease when the Ta contents 10.6 Vol%. This could be attributed to the presence of comparatively larger clusters of Ta particles and obvious voids. The agglomeration of HA particles may lead to weak combination and grain boundary embrittlement thus reducing the strengths of the composites.

At 10.6 Vol% Ta content most of the particle clusters in the composite. So it is also likely to reduce the contribution of Orowan strengthening in the composite with 10.6 Vol% Ta once the clusters grow beyond a critical size [125].

In the present work, the maximum improvement of strength was obtained in the case of the addition amount of 6.9 Vol% Ta. On the other hand, increase in the elastic moduli of the composites containing 3.3 and6.9 Vol% Ta can be attributed to the presence of:

(a) The high modulus of reinforcement;

(b) Uniform distribution of reinforcement with good interfacial integrity which leads to a significant increase in internal stress between reinforcement and matrix resulting in the enhancement of elastic modulus;

(c) The high loading transfer capacity of matrix–reinforcement interfaces [126,127].

Such defects as porosity may reduce the elastic modulus when the contents of Ta increase from 6.9 to 10.6 Vol% [127]. The elastic modulus (15.34 GPa) of the composites is close to that of human bone, suggesting that the Mg composites are promising candidates for implants to reduce stress shielding and bone absorption.

CHAPTER FIVE

5. CONCLUSION

In this study, Ta and HA particles reinforced magnesium matrix composites were synthesized by powder metallurgy technique. The fine Ta and HA particles uniformly distribute in the Mg matrices without voids for the composites containing 3.3 and 6.9 Vol% Ta. Strong interfacial bonding between Mg and reinforcement particles, with no chemical reaction and intermetallic phases, can be achieved. The shape and size of Mg powders were changed through mechanical milling. The presence of HA and Ta particles causes more reduction in size of Mg powders during the milling process. In Mg-reinforcement mixture powders, the transfiguration and reduced size of Mg powders improve the compressibility of the green compacts and attachment of particles during sintering process; resulting in low volume and small size of porosities in the composites. The addition of hybrid reinforcements significantly reduced the grain size and increased the hardness. The presence of minimal porosity can be related to the good compatibility between the matrix and reinforcement and proper selection of milling parameters. The ultimate compressive strengths, Failure strain and elastic moduli of the composites tend to increase when the Ta contents increase from 0 to 6.9 Vol%, however, appear to decrease with the further increase of Ta from 6.9 to 10.6 Vol%. But the yield strength was increased when the Ta content increased from 6.9 to 10.6 Vol%.

References

[1] C. Suryanarayana, N. Al-Aqeeli /- Mechanically alloyed nanocomposites. Progress in Materials Science 58 (2013) 383–502

[2] Miracle DB. Metal matrix composites – from science to technological significance. Compos Sci Technol 2005; 65:2526–40.

[3] Tjong SC. Novel nanoparticle-reinforced metal matrix composites with enhanced mechanical properties. Adv Eng Mater 2007; 9:639–52.

[4] Tjong SC. Novel nanoparticle-reinforced metal matrix composites with enhanced mechanical properties. Adv Eng. Mater 2007; 9:639–52.

[5] Buddy D. Ratner, Allan S. Hoffman, Frederick J. Schoen, Jack E. Lemons/ An Introduction to Materials in Medicine. Third Edition. Page no.841-853

[6] Niinomi M. Recent metallic materials for biomedical applications. Met Mater Trans A 2002; 33:477–86.

[7] DeGarmo PE. Materials and processes in manufacturing, 5th ed. New York: Collin Macmillan; 1979: 103-154

[8] Water, electrolyte mineral and acid/base metabolism. Section 2. Endocrine & Metabolic Disorders. Merk Manual of Diagnosis and Therapy :203-276

[9] Saris NEL. Magnesium: an update on physiological, clinical and analytical aspects. Clin Chim Acta 2000; 294:1–26.

[10] Okuma T. Magnesium and bone strength. Nutrition 2001; 17:679–80.

[11] Vormann J. Magnesium: nutrition and metabolism. Mol Aspects Med 2003; 24:27–37.

[12] Wolf FI, Cittadini A. Chemistry and biochemistry of magnesium. Mol Aspects Med 2003; 24:3–9.

[13] Hartwig A. Role of magnesium in genomic stability. Mutat Res/Fund Mol Mech Mutagen 2001; 475:113–2.

[14] Revell PA, Damien E, Zhang XS, Evans P, Howlett CR. The effect of mangesium ions on bone bonding to hydroxyapatite. Key Eng Mater 2004;254–256:447–50.

[15] Zreiqat H, Howlett CR, Zannettino A, Evans P, Schulze-Tanzil G, Knabe C, et al. Mechanisms of magnesium-stimulated adhesion of osteoblastic cells to commonly used orthopedic implants. J Biomed Mater Res 2002; 62:175–84.

[16] Yamasaki Y, Yoshida Y, Okazaki M, Shimazu A, Uchida T, Kubo T, et al. Synthesis of functionally graded MgCO3 apatite accelerating osteoblast adhesion. J Biomed Mater Res 2002; 62:99–105.

[17] Yamasaki Y, Yoshida Y, Okazaki M, Shimazu A, Kubo T, Akagawa Y, et al. Action of FG-MgCO3 Ap-collagen composite in promoting bone formation. Biomaterials 2003; 24:4913–20

[18] Witte F, Kaese V, Haferkamp H, Switzer E, Meyer-Lindenberg A, Wirth CJ, et al. In vivo corrosion of four magnesium alloys and the associated bone response. Biomaterials 2005; 26:3557–63.

[19] Lambotte A. L'utilisation du magnesium comme materiel perdu dans l'osteosynthe`se. Bull Me´m Soc Nat Chir 1932; 28:1325–34.

[20] Troitskii VV, Tsitrin DN. The resorbing metallic alloy 'Osteosinthezit' as material for fastening broken bone. Khirurgiia 1944; 8:41–4

[21] Y.L. Zhou, D.M. Luo, W.Y. Hu, Y.C. Li, P. Hodgson, C.E. Wen, in: Proceedings of the 2nd International Conference on Manufacturing Science and Engineering, ICMSE 2011, Advanced Materials Research, Guilin; China, pp. 56–59, 2011.

[22] Y. Ding, C. Wen, P. Hodgson, Y. Li, J. Mater. Chem. B 2 (2014) 1912–1933.

[23] Y. Li, C. Wen, D. Mushahary, R. Sravanthi, N. Harishankar, G. Pande, P. Hodgson, Acta Biomater. 8 (2012) 3177–3188.

[24] D. Persaud-Sharma, A. McGoron, J. Biomim. Biomater. Tissue Eng. 12 (2012) 25–39.

[25] M.P. Staiger, A.M. Pietak, J. Huadmai, G. Dias, Biomaterials 27 (2006) 1728–1734.

[26] F. Witte, Acta Biomater. 6 (2010) 1680–1692

[27] A. Daoud, M.T.A. El-khair, M. Abdel-Aziz, P. Rohatgi, Compos. Sci. Technol. 67 (2007) 1842–1853.

[28] M. Mabuchi, K. Kubota, K. Higashi, Scr. Metall. Et. Mater. 33 (1995) 331–335.

[29] A. Feng, Y. Han, Mater. Des. 32 (2011) 2813–2820.

[30] M. Nakach, J.R. Authelin, A. Chamayou, J. Dodds, Comparison of various milling technologies for grinding pharmaceutical powders, International Journal of Mineral Processing 74 (2004) S173–S181.

[31] M. He, Y. Wang, E. Forssberg, Slurry rheology in wet ultrafine grinding of industrial minerals: a review, Powder Technology 147 (2004) 94–112.

[32] L. Takacs, Self-sustaining reactions induced by ball milling, Progress in Materials Science 47 (2002) 355–414.
[33] Weeber AW, Bakker H, deBoer FR. The preparation of amorphous Ni–Zr powder by grinding the crystalline alloy. Europhys Lett 1986; 2:445–8.
[34] Alireza Vahid, Peter Hodgson, Yuncang Li, Materials Science & Engineering A 685 (2017) 349–357.
[35] W.F. Gale, T.C. Totemeier, Smithells metals reference book, Butterworth Heinemann, 2003.
[36] M.M. Avedesian, H. Baker, Magnesium and Magnesium Alloys-ASM Speciality Handbook, ASM International, Ohio, 1999 (53-104)
[37] J. Willekens, Magnesium–Verfu¨gbarkeit, Markttendenzen, Preisentwicklung DGM-Fortbildungsseminar, Clausthal-Zellerfeld, 29, 31.10.1997.
[38] Gibson L, Ashby M. Cellular solids. Structure and properties. Sydney: Pergamum Press; 1988. p. 1–41.
[39] Gibson L, Ashby M. Cellular solids. Structure and properties. Sydney: Pergamum Press; 1988. p. 316–331.
[40] Choi JW, Kong YM, Kim HE, Lee IS. Reinforcement of hydroxyapatite bio ceramic by addition of Ni3Al and Al2O3. J Am Ceram Soc 1998; 81:1743–91.
[41] Thamaraiselvi TV, Rajeswari S. Biological evaluation of bio ceramic materials—a review. Trends Biomater Artif Organs 2004; 19:9–17.
[42] B.L. Mordike, T. Ebert. Magnesium Properties — applications — potential. Materials Science and Engineering A302 (2001) 37–45.
[43] Y. Li, M. Li, W. Hu, P. Hodgson, C. Wen, in: Proceedings of the in: Procedings of the 7th Pacific Rim International Conference on Advanced Materials and Processing, PRICM-7, Materials Science Forum, Cairns, QLD; Australia, pp. 2192– 2195, 2010.
[44] H.E. Friedrich, B.L. Mordike, Magn. Metall. Technol.: Metall. Des. Data, Appl. (2006) (V-VI):675-736
[45] Y. Li, C. Wen, D. Mushahary, R. Sravanthi, N. Harishankar, G. Pande, P. Hodgson, Acta Biomater. 8 (2012) 3177–3188.
[46] Li Z, Gu X, Lou S, Zheng Y. The development of binary Mg–Ca alloys for use as biodegradable materials within bone. Biomaterials 2008; 29:1329–44
[47] Gu X, Zheng Y, Cheng Y, Zhong S, Xi T. In vitro corrosion and biocompatibility of binary magnesium alloys. Biomaterials 2009; 30:484–98.

[48] Xu L, Pan F, Yu G, Yang L, Zhang E, Yang K. In vitro and in vivo evaluation of the surface bioactivity of a calcium phosphate coated magnesium alloy. Biomaterials 2009; 30:1512 23.

[49] Pietak A, Mahoney P, Dias GJ, Staiger MP. Bone-like matrix formation on magnesium and magnesium alloys. J Mater Sci Mater Med 2008; 19:407–15.

[50] Xu L, Zhang E, Yang K. Phosphating treatment and corrosion properties of Mg– Mn–Zn alloy for biomedical application. J Mater Sci-Mater Med 2009; 20:859–67.

[51] Wen C, Guan S, Peng L, Ren C, Wang X, Hu Z. Characterization and degradation behavior of AZ31 alloy surface modified by bone-like hydroxyapatite for implant applications. Appl Surf Sci 2009; 255:6433–8.

[52] Song YW, Shan DY, Han EH. Electrodeposition of hydroxyapatite coating on AZ91D magnesium alloy for biomaterial application. Mater Lett 2008; 62:3276–9.

[53] Witte F, Feyerabend F, Maier P, Fischer J, Stormer M, Blawert C, et al. Biodegradable magnesium-hydroxyapatite metal matrix composites. Biomaterials 2007; 28:2163–74

[54] Witte F, Ulrich H, Rudert M, Willbold E. Biodegradable magnesium scaffolds: part I: appropriate inflammatory response. J Biomed Mater Res Part A 2007;81A:748–56.

[55] Landgraeber S, von Knoch M, Loer F, Wegner A, Tsokos M, Hussmann B, et al. Extrinsic and intrinsic pathways of apoptosis in aseptic loosening after total hip replacement. Biomaterials 2008; 29:3444–50

[56] M. Shanthi, P. Jayaramanavar, V. Vyas, D.V.S. Seenivasan, M. Gupta, J. Alloy. Compd. 513 (2012) 202–207.

[57] D.J. Lloyd, Int. Mater. Rev. 39 (1994) 1–23.

[58] F. Moll, K. Kainer, Magnes. -Alloy. Technol. (2002) 197–217.

[59] S.F. Hassan, M. Gupta, Development of ductile magnesium composite materials using titanium as reinforcement, J. Alloys Compd. 345 (2002) 246–251

[60] Junko Umeda, Masashi Kawakami, Katsuyoshi Kondoh, EL-Sayed Ayman, Hisashi Imai. / Materials Chemistry and Physics 123 (2010) 649–657

[61] Y.L. Xi, D.L. Chai, W.X. Zhang, J.E. Zhou, Titanium alloy reinforced magnesium matrix composite with improved mechanical properties, Scripta Mater. 54 (2006) 19–23.

[62] M. Shanthi, P. Jayaramanavar, V. Vyas c, D.V.S. Seenivasan, M. Gupta. Journal of Alloys and Compounds 513 (2012) 202–207

[63] Niinomi M. Recent metallic materials for biomedical applications. Met Mater Trans A 2002; 33:477–86.
[64] Puleo DA, Huh WW. Acute toxicity of metal ions in cultures of osteogenic cells derived from bone marrow stromal cells. J Appl Biomater 1995; 6:109–16.
[65] Nagels J, Stokdijk M, Rozing PM. Stress shielding and bone resorption in shoulder arthroplasty. J Shoulder Elbow Surg 2003; 12:35–9.
[66] Mark P. Staiger, Alexis M. Pietak, Jerawala Huadmaia, George Dias. Biomaterials 27 (2006) 1728 –1734.
[67] Y. Wang, J. Huang, Texture analysis in hexagonal materials, Mater. Chem. Phys. 81 (2003) 11e26.:123-231
[68] G.E. Dieter, Mechanical Metallurgy, McGraw-Hill, New York, 1976.
[69] D. Lloyd, Particle reinforced aluminum and magnesium matrix composites, Int. Mater. Rev. 39 (1994) 1e23.
[70] M. Handbook, Properties and Selection of Metals, vol. 1, American Society for Metals, 1961, p. 1206.
[71] S. Sankaranarayanan, R.K. Sabat, S. Jayalakshmi, S. Suwas, M. Gupta. Materials Chemistry and Physics 143 (2014) 1178-1190.
[72] Pietak A, Mahoney P, Dias GJ, Staiger MP. Bone-like matrix formation on magnesium and magnesium alloys. J Mater Sci Mater Med 2008; 19:407–15.
[73] Yun Y, Dong Z, Yang D, Schulz MJ, Shanov VN, Yarmolenko S, et al. Biodegradable Mg corrosion and osteoblast cell culture studies. Mater Sci Eng C 2009;29:1814–21.
[74] Song G, Song S. A possible biodegradable magnesium implant material. Adv Eng Mater 2007;9:298–302.
[75] Ailing Feng, Yong Han. Materials and Design 32 (2011) 2813–2820.
[76] Chen, Y.; Xu, Z.; Smith, C.; Sankar, J. Recent advances on the development of magnesium alloys for biodegradable implants. *Acta Biomater.* **2014**, *10*, 4561–4573.
[77] Khin Sandar Tun, Wai Leong Eugene Wong, Quy Bau Nguyen and Manoj Gupta. Tensile and Compressive Responses of Ceramic and Metallic Nanoparticle Reinforced Mg Composites. Materials 2013, 6.
[78] Doležal, P.; Zapletal, J.; Fintov á, S.; Trojanov á, Z.; Greger, M.; Roupcov á, P.; Podr ábsk ý, T. Influence of processing techniques on microstructure and mechanical properties of a biodegradable Mg-3Zn-2Ca alloy. Materials 2016, 9, 880.
[79] Chun Chiu, Chih-Te Lu, Shih-Hsun Chen and Keng-Liang Ou. Effect of Hydroxyapatite on the Mechanical Properties and Corrosion Behavior of Mg-Zn-Y Alloy *Materials* 2017, *10*, 855.
[80] Frank Witte. The history of biodegradable magnesium implants. Acta Biomaterial 6 (2010) 1680–1692.

[81] H.E. Friedrich, B.L. Mordike, Magn. Metall. Technol.: Metall. Des. Data, Appl. (2006) (V-VI).

[82] F. Chmelík, F. Moll, J. Kiehn, P. Lukáč, B.L. Mordike, K.U. Kainer, Adv. Eng. Mater. 2 (2000) 600–604.

[83] M. Gupta and G.K. Meenashisundaram, Insight into Designing Biocompatible. Synthesis of Magnesium-Based Biomaterials (2015).

[84] M.K. Jain, V.V. Bhanuprasad, S.V. Kamat, A.B. Pandey, V.K. Varma, B.V.R. Bhat, Y. Mahajan, Int. J. Powder Metall. 29 (1993) 267.

[85] J.J. Lewandowski, C. Liu, W.H. Hunt Jr, in: P. Kumar et al. (Eds.), Processing and Properties for Powder Metallurgy Composites, TMS/AIME, Warrendale, PA, 1987, p. 117.

[86] M.J. Tan, X. Zhang. Powder metal matrix composites: selection and processing Materials Science and Engineering A244 (1998) 80–85.

[87] Karl U. Kainer, Metal Matrix Composites: Custom made Materials for Automotive and Aerospace Engineering, Wiley, 2006

[88] S. Sankaranarayanan, S. Jayalakshmi, M. Gupta. Journal of Alloys and Compounds 509 (2011) 7229–7237.

[89] C. Suryanarayana, E. Ivanov, and V. Boldyrev, "The science and technology of mechanical alloying," *Mater. Sci. Eng. A*, vol. 304–306, pp. 151 –158, 2001.

[90] Y. Yang, P. Wu, Q. Wang, H. Wu, Y. Liu, Y. Deng, Y. Zhou, and C. Shuai, "The Enhancement of Mg Corrosion Resistance by Alloying Mn and Laser-Melting," *Materials (Basel).*, vol. 9, no. 4, p. 216, 2016.

[91] B.L. Mordike, P. Lukác, Physical metallurgy, in: H.E. Friedrich, B.L. Mordike (Eds.), Magnesium Technology: Metallurgy, Design Data, Applications, Springer, New York, 2006, p. 63.

[92] V.S. Zolotorevsky, N.A. Belov, M.V. Glazoff, Casting Aluminium Alloys, Elsevier, Amsterdam, 2007.

[93] M. Mabuchi, H. Iwasaki, K. Yanase, K. Higashi, Scripta Materialia 36 (1997) 681.

[94] Z.L. Pei, K. Li, J. Gong, N.L. Shi, E. Elangovan, C. Sun, Journal of Materials Science 44 (2009) 4124.

[95] Hiroyuki Fukuda, Katsuyoshi Kondoh, Junko Umeda, Bunshi Fugetsu. Materials Chemistry and Physics 127 (2011) 451–458.

[96] S. Jayalakshmi, Shreyasi Sahu, S. Sankaranarayanan, Sujasha Gupta, M. Gupta. Materials and Design 53 (2014) 849–855.

[97] M. Razavi, M.H. Fathi, M. Meratian. Materials Science and Engineering A 527 (2010) 6938–6944.

[98] Witte F, Fischer J, Nellesen J, Crostack H, Kaese V, Pischd A, et al. In vitro and in vivo corrosion measurements of magnesium alloys. Biomaterials 2006;27:1013–8.
[99] Li ZJ, Gu XN, Lou SQ, Zheng YF. The development of binary Mg–Ca alloys for use as biodegradable materials within bone. Biomaterials 2008;29(10):1329–44.
[100] Xu LP, Yu GN, Zhang EL, Pan F, Yang K. In vivo corrosion behavior of Mg–Mn–Zn alloy for bone implant application. J Biomed Mater Res 2007;83A(3):703–11.
[101] Y.F. Zheng, X.N. Gu, Y.L. Xi, D.L. Chai. In vitro degradation and cytotoxicity of Mg/Ca composites produced by powder metallurgy Acta Biomaterial 6 (2010) 1783–1791.
[102] K.K. Chawla, Ceramic Matrix Composites, Springer, 1998.
[103] K. Chawla, Rev. Bras. De. Física 4 (1974) 411–418.
[104] S.C. Sharma, J. Mater. Eng. Perform. 12 (2003) 324–330.
[105] Wen, M. Mabuchi, Y. Yamada, K. Shimojima, Y. Chino, T. Asahina, Scr. Mater. 45 (2001) 1147–1153.
[106] A. Nouri, C. Wen, Crit. Rev. Solid State Mater. Sci. 39 (2014) 81–108
[107] Č. J, D. Vojtěch, Mater. Sci. Eng.: C 33 (2013) 564–569.
[108] D. Taarea, S.I. Bakhtiyarov, 14 - General physical properties, in: W.F.G.C. Totemeier (Ed.) Smithells Metals Reference Book Eighth edition, Butterworth-Heinemann, Oxford, 2004, pp. 1–45
[109] Zhong XL, Wong WLE, Gupta M. Enhancing strength and ductility of magnesium by integrating it with aluminum nanoparticles. Acta Mater 2007; 55:6338–44.
[110] A. Handbook, Ed. Dieter, EG ASM, Materials Park, OI-I, 998 (1997).
[111] T.B. Massalski, H. Okamoto, P. Subramanian, L. Kacprzak, W.W. Scott, Binary alloy phase diagrams, Am. Soc. Met. Met. Park, OH (1986).
[112] A.A. Nayeb-Hashemi, J.B. Clark, A.S.M. International, Phase diagrams of binary magnesium alloys, ASM International, Metals Park, Ohio, 1988.
[113] Chua BW, Lu L, Lai MO. Influence of SiC particles on mechanical properties of Mg based composite. Compos Struct 1999; 47:595–601.
[114] Y. Shimizu, S. Miki, T. Soga, I. Itoh, H. Todoroki, T. Hosono, K. Sakaki, Y.A. Kim, Scripta Mater. 58 (2008) 267–270.
[115] L. Lu, C.Y.H. Lim, W.M. Yeong, Compos. Struct. 66 (2004) 41–45.
[116] G. Meijer, F. Ellyin, Z. Xia, Composites B 31 (2000) 29–37.

[117] X. Gu, W. Zhou, Y. Zheng, L. Dong, Y. Xi, D. Chai, doi:10.1016/ j.msec.2010.03.016.

[118] C. Suryanarayana, Prog. Mater. Sci. 46 (2001) 1–184.

[119] P.S. Gilman, J.S. Benjamin, Annu. Rev. Mater. Sci. 13 (1983) 279–300.

[120] D.J. Lloyd, Int. Mater. Rev. 39 (1994) 1–23.

[121] T.C. Tszeng, Compos. Part B: Eng. 29 (1998) 299–308.

[122] Habibnejad-Korayem M, Mahmudi R, Poole WJ. Enhanced properties of Mgbased nano-composites reinforced with Al2 O3 nano-particles. Mater Sci Eng A 2009; 519:198–203.

[123] Goh CS, Wei J, Lee LC, Gupta M. Development of novel carbon nanotube reinforced magnesium nanocomposites using the powder metallurgy technique. Nanotechnology 2006; 17:7–12.

[124] Hassan SF, Gupta M. Development of ductile magnesium composite materials using titanium as reinforcement. J Alloys Compd 2002; 345:246–51.

[125] Wong WLE, Gupta M. Development of Mg/Cu nanocomposites using microwave assisted rapid sintering. Compos Sci Technol 2007; 67:1541–52.

[126] Hassan SF, Gupta M. Development of high performance magnesium nanocomposites using nano-Al2 O3 as reinforcement. Mater Sci Eng A 2005; 392:163–8.

[127] Xi YL, Chai DL, Zhang WX, Zhou JE. Titanium alloy reinforced magnesium matrix composite with improved mechanical properties. Scr Mater 2006; 54:19–23.